Circulation Research

ORIGINAL RESEARCH

GSK3β Deficiency Expands Obese Adipose Vasculature to Mitigate Metabolic Disorders

Li Wang, Jiajia Li, Ping Tang, Dongliang Zhu, Lixin Tai, Yuan Wang, Tsukiko Miyata, James R. Woodgett, Li-jun Di

BACKGROUND: Maintaining a well-developed vascular system alongside adipose tissue (AT) expansion significantly reduces the risk of metabolic complications. Although GSK3β (glycogen synthase kinase-3 beta) is known for its role in various cellular processes, its specific functions in AT and regulation of body homeostasis have not been reported.

METHODS: GSK3β-floxed and GSK3α-floxed mice were crossed with adiponectin-Cre mice to generate GSK3β or GSK3α adipocyte-specific knockout mice ($GSK3\beta^{ADKO}$ and $GSK3\alpha^{ADKO}$). A comprehensive whole-body metabolism analysis was performed on obese $GSK3\beta^{ADKO}$ mice induced by a high-fat diet. RNA sequencing was conducted on AT of both obese $GSK3\beta^{ADKO}$ and $GSK3\alpha^{ADKO}$ mice. Various analyses, including vessel perfusion studies, lipolysis analysis, multiplex protein assays, in vitro protein phosphorylation assays, and whole-mount histology staining, were performed on AT of obese $GSK3\beta^{ADKO}$ mice. Tube-formation experiments were performed using 3B-11 endothelial cells cultured in the conditional medium of matured adipocytes under hypoxic conditions. Chromatin precipitation and immunofluorescence studies were conducted using cultured adipocytes with GSK3 inhibition.

RESULTS: Our findings provide the first evidence that adipocyte-specific knockout of GSK3β expands AT vascularization and mitigates obesity-related metabolic disorders. GSK3β deficiency, but not GSK3α, in adipocytes activates AMPK (AMP-activated protein kinase), leading to increased phosphorylation and nuclear accumulation of HIF-2α, resulting in enhanced transcriptional regulation. Consequently, adipocytes increased VEGF (vascular endothelial growth factor) expression, which engages VEGFR2 on endothelial cells, promoting angiogenesis, expanding the vasculature, and improving vessel perfusion within obese AT. GSK3β deficiency promotes AT remodeling, shifting unhealthy adipocyte function toward a healthier state by increasing insulin-sensitizing hormone adiponectin and preserving healthy adipocyte function. These effects lead to reduced fibrosis, reactive oxygen species, and ER (endoplasmic reticulum) stress in obese AT and improve metabolic disorders associated with obesity.

CONCLUSIONS: Deletion of GSK3β in adipocytes activates the AMPK/HIF-2α/VEGF/VEGFR2 axis, promoting vasculature expansion within obese AT. This results in a significantly improved local microenvironment, reducing inflammation and effectively ameliorating metabolic disorders associated with obesity.

Key Words: glycogen synthase kinase 3 beta ■ obesity ■ vascular endothelial growth factor A

Meet the First Author, see p 3 | Editorial, see p 112

Adipose tissue (AT) displays remarkable plasticity, undergoing rapid and dynamic expansion or contraction in response to changes in energy intake, thereby maintaining systemic energy metabolism balance.[1] Sufficient and well-organized vascularization is critical for tissue expansion and proper physiological function. This vital process is accomplished through angiogenesis, which entails the formation of new blood vessels derived from preexisting ones.[2–4] In obese AT, decoupling of angiogenesis and adipogenesis leads to

Correspondence to: Lijun Di, PhD, Faculty of Health Sciences, University of Macau, Avenida da Universidade, Taipa, Macau SAR, China, Email lijundi@um.edu.mo; or Li Wang, PhD, Faculty of Health Sciences, University of Macau, Avenida da Universidade, Taipa, Macau SAR, China, Email liwang@um.edu.mo
Supplemental Material is available at https://www.ahajournals.org/doi/suppl/10.1161/CIRCRESAHA.124.325187.
For Sources of Funding and Disclosures, see page 109.

Circulation Research is available at www.ahajournals.org/journal/res

ORIGINAL RESEARCH

Novelty and Significance

What Is Known?

- GSK3β (glycogen synthase kinase-3 beta) is important in many key cellular functions, and it plays a regulatory role in the activity of glycogen synthase in muscle, influencing insulin activity.
- GSK3β in the liver has shown no significant impact on insulin resistance and glucose metabolism.
- VEGF (vascular endothelial growth factor), predominantly secreted by adipocytes, regulates the vasculature in adipose tissue and maintains adipose tissue homeostasis.

What New Information Does This Article Contribute?

- The deletion of GSK3β in adipocytes improves the microenvironment of obese adipose tissue and restores metabolic health associated with obesity by inducing the expansion of adipose vasculature.
- The deficiency of GSK3β in adipocytes affects adipocyte size and promotes healthy expansion of subcutaneous adipose tissue.
- Deletion of GSK3β in adipocytes activates AMPK (AMP-activated protein kinase), promoting nuclear accumulation of HIF-2α (hypoxia-inducible factor 2-alpha) and enhancing its transcriptional regulatory effect on VEGF, ultimately stimulating adipose tissue vascularization through VEGF/VEGFR2 signaling.

The precise role of GSK3β in adipose tissue and its effects on the tissue microenvironment and metabolic balance remain largely elusive. Our research unveils the novel GSK3β/AMPK/HIF-2α/VEGF/VEGFR2 pathway in adipose tissue, demonstrating that GSK3β depletion in adipocytes triggers the AMPK/HIF-2α/VEGF/VEGFR2 axis, mediating communication between adipocytes and endothelial cells and promoting vasculature expansion in obese adipose tissue. This leads to a healthier local environment, marked by reduced hypoxia, fibrosis, and ER stress. Notably, GSK3β deficiency in adipocytes results in smaller adipocytes and a beneficial expansion of subcutaneous white adipose tissue compared with epididymal white adipose tissue, leading to reduced adipose inflammation and improved insulin sensitivity. Our study not only uncovers GSK3β's role in adipose tissue but also highlights its function in mediating adipocyte-endothelial cell interactions in obese adipose tissue. This interplay exerts precise control over local vascularity and improves the adipose tissue microenvironment, highlighting a potential path for the restoration of metabolic health within the setting of obesity.

Nonstandard Abbreviations and Acronyms

AMPK	AMP-activated protein kinase
AT	adipose tissue
DEG	differentially expressed gene
eWAT	epididymal white adipose tissue
GSK3ß	glycogen synthase kinase-3 beta
HFD	high-fat diet
HIF-2α	hypoxia-inducible factor 2-alpha
LPL	lipoprotein lipase
OxPhos	oxidative phosphorylation
PPARγ	peroxisome proliferator-activated receptor gamma
qRT-PCR	quantitative reverse transcription polymerase chain reaction
RNA-seq	RNA sequencing
ROS	reactive oxygen species
sWAT	subcutaneous white adipose tissue
SVF	stromal vascular fraction
UCP1	uncoupling protein 1
VEGF	vascular endothelial growth factor
WAT	white adipose tissue

insufficient vascularity,[2–5] which reduces blood flow to AT. Chronic obesity caused by uncontrolled tissue expansion triggers some pathological changes, including hypoxia, reactive oxygen species (ROS) production, endoplasmic reticulum stress, fibrosis, and adipocyte necrosis/apoptosis.[6–11] These changes, especially hypoxia, play causal roles in AT dysfunction, the development of insulin resistance, immune cell infiltration, and inflammation, which contribute to the development of metabolic disorders.[12–14]

The concurrent development of a well-established vascular system with AT expansion significantly improves the local hypoxic condition, diminishes oxidative stress, mitigates inflammation, and consequently reduces the risk of insulin resistance and the onset of type 2 diabetes.[12,13] The beneficial effects of induced vascularization have been demonstrated in both early and late stages of metabolic diseases.[13,15,16] Therefore, vascularity is considered a rate-limiting step in maintaining internal homeostasis of AT in different physiological and pathological states.[12,17]

Previous studies have shown that AT regulates angiogenesis and automatically induces vascular remodeling. Adipocytes have been reported to secrete several angiogenic factors, such as adiponectin, leptin, hepatocyte growth factor 1, angiopoietin, and VEGF (vascular endothelial growth factor). These factors act on the

vascular endothelial cells in AT to regulate angiogenesis.[17–19] VEGF is responsible for the majority of angiogenic activity in AT.[5,17] Adipocyte-secreted VEGF works through VEGFR2, one of the VEGF receptors, mainly expressed by vascular endothelial cells, to regulate angiogenesis in a paracrine manner.[16,20] The level of VEGF has been found to decrease in the AT of obese humans.[21,22] Inducing the release of VEGF by adipocytes activates the VEGF/VEGFR signaling pathway and stimulates AT vasculature to counteract obesity-associated metabolic disorders.[16,20,23,24] Therefore, effective communication between adipocytes and endothelial cells within AT is essential for maintaining a stable tissue microenvironment, which can have considerable impacts on metabolic complications.

GSK3 is a serine/threonine kinase that inhibits glycogen synthase activity and has a wide range of biological functions.[25–28] Both GSK3α and GSK3β are widely expressed in all mammalian cells, and they participate in many metabolism- and glucose-homeostasis-related signaling pathways.[29–31] Improved insulin resistance and increased glucose tolerance have been observed in mice with whole-body knockout of GSK3α. However, these effects are not attributed to the knockout of GSK3α in the liver or muscle, as liver- or muscle-specific GSK3α knockout animals do not elicit similar effects.[32,33] Whole-body GSK3β knockout in mice is lethal, and muscle-specific knockout in mice have shown that GSK3β mainly regulates glycogen synthase activity and insulin activity in muscles.[34] In the liver, GSK3β has no significant effect on insulin resistance or glucose metabolism.[29] It remains an open question how other tissue-specific functions of GSK3 isoforms play a role in regulating metabolism and insulin activity. Our recent study has demonstrated that the systemic, small-molecule-mediated inhibition of GSK3 reduces obesity-related chronic inflammation through the regulation of macrophage subtypes in AT to improve insulin resistance.[35] To date, no study has investigated the specific functions of GSK3 isoforms in AT or how GSK3 affects the AT microenvironment and metabolic homeostasis. GSK3 was proposed to be a promising therapeutic target for various diseases, and some GSK3 inhibitors have been studied in clinical trials,[36,37] but GSK3 inhibitors have yet to be applied in clinical settings. This is primarily attributable to the fact that most GSK3 inhibitors simultaneously inhibit both GSK3α and GSK3β isoforms, which may cause severe side effects. Recent studies have suggested that, compared with nonselective inhibitors, GSK3-isoform-selective inhibitors are more effective in the treatment of certain diseases, such as acute myeloid leukemia and fragile X syndrome, with less side effects,[38,39] indicating that the development and optimization of GSK3-selective inhibitors for treating related diseases may have broad prospects for clinical application. Therefore, it is critical to fully understand tissue-specific functions of GSK3 isoforms. Here, we have explored the adipocyte-specific functions of GSK3β, most notably its biological and pathophysiological roles in high-fat diet (HFD)-induced obese AT. We observed reduced inflammation, improved insulin sensitivity, and a more favorable microenvironment in the AT of mice with adipocyte-specific GSK3β deletion. Mechanistically, we demonstrated that GSK3β deficiency increased AMPK (AMP-activated protein kinase) activity to stimulate HIF-2α (hypoxia-inducible factor 2-alpha) phosphorylation and nuclear accumulation, increasing the expression of its target gene, *VEGF*, in adipocytes. VEGF then binds to VEGFR2 expressed on endothelial cells to promote vascularization and increase perfusion of AT, thereby alleviating obesity-associated metabolic disorders.

METHODS

Data Availability

The authors declare that all data are accessible both within the article and in the accompanying Supplemental Material. A detailed description of the Methods and Materials can be found in the "Methods and Materials" section of the Supplemental Material. The Major Resources Table is also included in the Supplemental Material. Any additional supporting data from this study and the required analytical tools can be obtained from the corresponding author upon reasonable request.

RESULTS

Systemic Inhibition of GSK3 Results in Transcriptional Upregulation of Angiogenesis-Associated Genes and Expanded Vascularity

We analyzed the RNA sequencing (RNA-seq) data obtained from epididymal white adipose tissue (eWAT) of obese mice treated with the highly potent and ATP-competitive GSK3 inhibitor SB216763 (SB).[35,40,41] To assess the impact of the treatment, we compared this data set with the RNA-seq data obtained from obese eWAT samples without or with SB treatment. Of the differentially expressed genes (DEGs) identified from obese+SB versus obese, 137 were upregulated and 847 were downregulated ($P<0.05$, log2 FC>log2(2); Figure S1A). Angiogenesis-associated gene ontology terms were predominant among the upregulated DEGs in the eWAT of SB-treated obese mice compared with eWAT from obese control mice (Figure 1A). By analyzing the genes upregulated by SB using gene set enrichment analysis, the gene functions associated with the positive regulation of angiogenesis were among the top hits (Figure S1B). Angiogenesis marker genes, including *VEGF*, *VEGFb*, *Kdr* (VEGFR2), and *PECAM1* (CD31), were upregulated, as indicated by the heat map analysis (Figure S1C), suggesting that GSK3 inhibition may stimulate angiogenesis in obese eWAT. The upregulated expression of the angiogenesis marker genes *VEGF*, *VEGFb*, and their receptors was validated using quantitative reverse transcription polymerase chain reaction

ORIGINAL RESEARCH

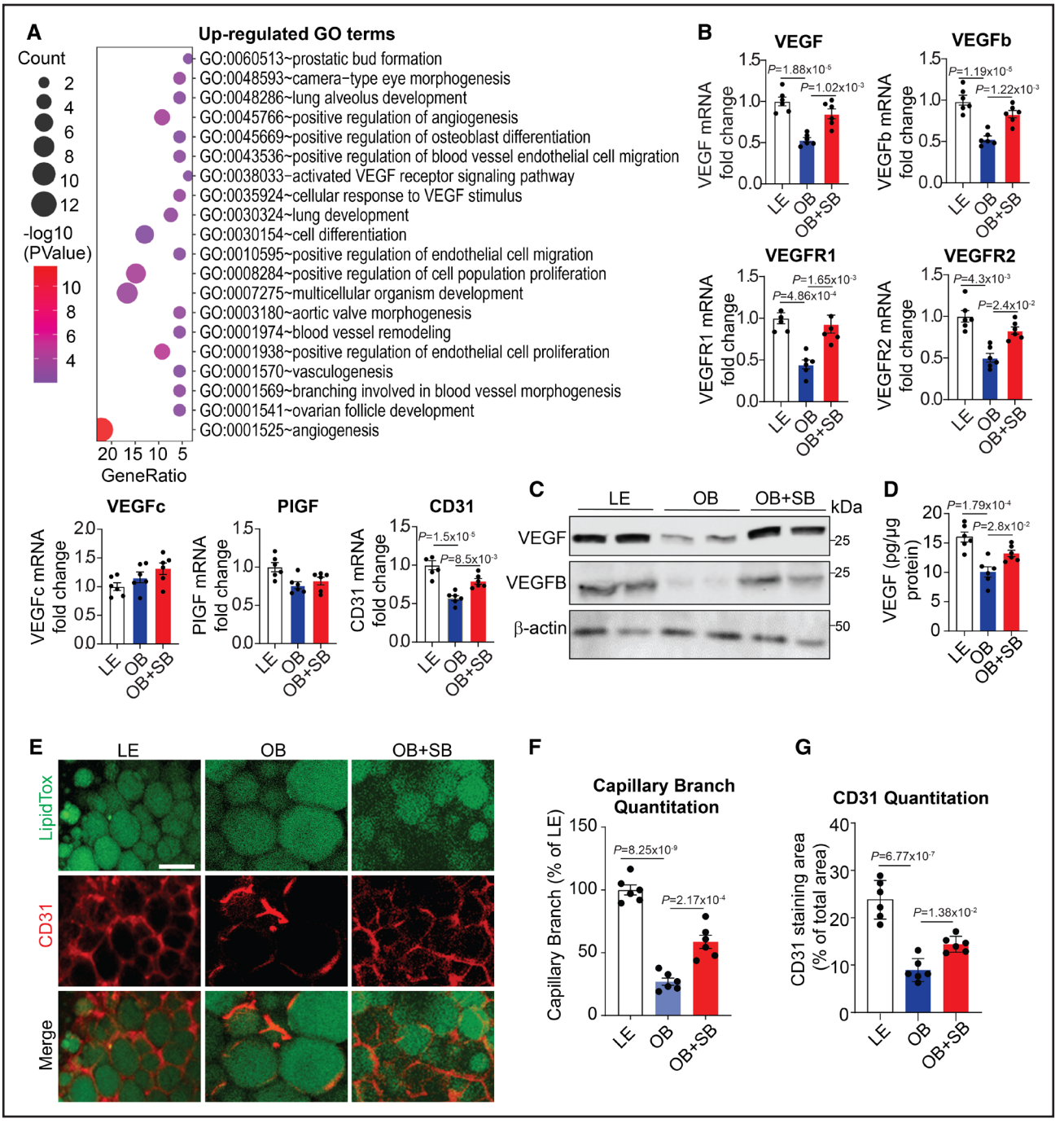

Figure 1. GSK3 (glycogen synthase kinase-3) inhibition stimulates vasculature expansion in adipose tissue of obese mice. Male C57Bl/6J lean mice (LE) were fed a normal chow diet, whereas male obese mice (OB) were fed a high-fat diet with or without SB216763 treatment (OB+SB). **A**, Gene ontology analysis showing upregulated gene signatures in the adipose tissue of the OB+SB mice vs OB mice (n=2). **B**, Quantification of the expression of angiogenesis marker genes in epididymal white adipose tissue (eWAT) from indicated mice using reverse transcription polymerase chain reaction (n=6). **C**, Western blotting analysis of VEGF (vascular endothelial growth factor) and VEGFB in eWAT from the indicated mice (n=6). **D**, ELISA assay of VEGF protein levels in eWAT from the indicated mice (n=6). **E** through **G**, Representative confocal microscope images of whole-mount CD31 staining in the indicated eWAT (**E**) and analysis for capillary branch density (**F**) and CD31-positive area (**G**) using ImageJ software (n=6). Scale bar=100 μm. **B**, **D**, **F**, and **G**, One-way ANOVA and Tukey post hoc test. PIGF indicates placental growth factor.

(RT-PCR; Figure 1B). Two other VEGF family members, *PIGF* (placental growth factor) and *VEGFc*, were unaffected by GSK3 inhibition (Figure 1B). SB treatment elevated VEGF and VEGFB protein levels in eWAT of obese mice (Figure 1C). VEGF protein increase in eWAT was validated by ELISA (Figure 1D). HFD reduced AT vascular density, but GSK3 inhibition significantly increased it, as evidenced by enhanced CD31 staining (Figure 1E

through 1G). These data support the idea that GSK3 negatively influences AT vascularization during obesity.

Adipocyte-Specific GSK3β Deficiency Improves Metabolic Complications

Considering that GSK3 inhibitor suppresses the activity of both GSK3α and GSK3β,[40] to further discern the potential influence of adipocyte-specific effects of GSK3 isoforms on AT vascularization during obesity, we generated mice with adipocyte-specific GSK3β deletion by mating chimeric GSK3β floxp/floxp (GSK3β$^{fl/fl}$) mice with another transgenic mice expressing an adiponectin promoter driving Cre recombinase gene to generate adipocyte-specific GSK3β knockout mice (GSK3β^{ADKO}).

GSK3β RNA loss was confirmed in white and brown AT, with a complete deletion in adipocytes (but not stromal vascular fraction [SVF] cells; Figure S2A). GSK3β protein levels were significantly reduced in eWAT and absent in adipocytes (Figure S2B). No compensatory increase in the GSK3α isoform was noted (Figure S2C).

Compared with control GSK3β$^{fl/fl}$ littermates, normal chow diet fed in both male and female GSK3β^{ADKO} mice showed no significant change in body weight (Figure S2D and S2E). A modest yet statistically significant reduction in body weight was observed in obese GSK3β^{ADKO} mice on HFD. The final body weights of male and female GSK3β^{ADKO} mice were recorded as 37.09 and 18.91 g, respectively, compared with control obese GSK3β$^{fl/fl}$ mice with final body weights of 42.7 g (male) and 23.57 g (female; Figure 2A and 2B; Figure S2F and S2G). After 22 weeks of HFD, GSK3β^{ADKO} mice had reduced fat mass compared with control littermates (Figure 2C; Figure S2H). Despite no change in food consumption on both normal chow diet

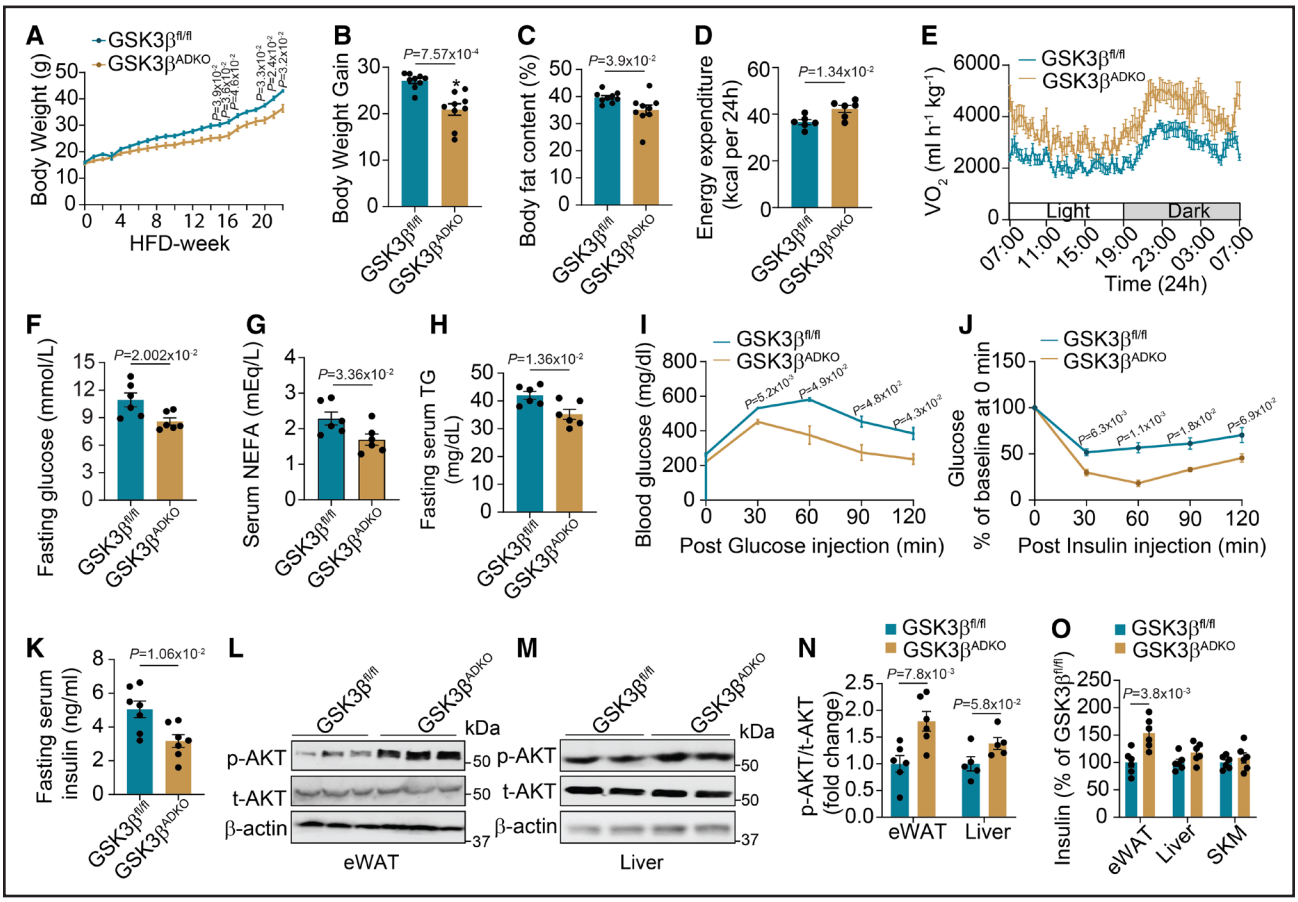

Figure 2. Adipocyte-specific GSK3β (glycogen synthase kinase-3 beta) deficiency alleviates obesity-associated metabolic complications and improves insulin signaling.
Male GSK3β$^{fl/fl}$ and GSK3β^{ADKO} mice were fed a high-fat diet (HFD) to induce obesity and used for the experiments. **A**, Body weight of male GSK3β$^{fl/fl}$ and GSK3β^{ADKO} mice fed an HFD (n=9). **B** through **H**, Comparison of body weight gain (**B**; n=9), body fat content (**C**; n=9), energy expenditure (**D**; n=6), oxygen consumption (**E**; n=6), fasting serum glucose (**F**; n=6), nonesterified fatty acid (NEFA; **G**; n=6), and triglyceride (TG) levels (**H**; n=6). **I** and **J**, Glucose tolerance test (**I**) and insulin tolerance test (**J**) of the indicated obese mice (n=6). **K**, Fasting serum insulin level of indicated obese mice (n=7). **L** through **N**, Western blotting images of AKT/PKB (AKT serine-threonine kinase/protein kinase B) phosphorylation (**L** and **M**) and quantification using ImageJ software (**N**) in epididymal white adipose tissue (eWAT) and the liver (n=6 for **L**; n=5 for **M**). **O,** ELISA analysis of the insulin level in different tissues from indicated obese mice (n=6). **A**, **I**, and **J**, Repeated ANOVA and Bonferroni post hoc test; **B** through **H**, **K**, **N** (eWAT), and **O**, 2-tailed unpaired *t* test; **N** (liver), nonparametric test. SKM indicates skeletal muscle.

and HFD conditions (Figure S2I), GSK3β deficiency notably improved metabolic traits, including increased energy expenditure and oxygen consumption (Figure 2D and 2E) and a nonsignificant increase in total activity (Figure S2J) of obese mice. GSK3β deficiency also enhanced the metabolic health of both male and female obese mice on HFD, as demonstrated by their low serum fasting glucose, triglyceride, and nonesterified fatty acid concentrations (Figure 2F through 2H; Figure S2K through S2M). No such changes were observed in the lean mice fed an normal chow diet (Figure S2N through S2P).

Moreover, GSK3β deficiency in adipocytes significantly reduced liver nonesterified fatty acid and triglyceride levels (Figure S3A and S3B) and increased LPL (lipoprotein lipase) mRNA levels in eWAT of obese mice (Figure S3C), consistent with improved lipid parameters. LPL expression and triglyceride levels in the heart remained unchanged (Figure S3C and S3D). The liver histology showed fewer and smaller lipid droplets (Figure S3E through S3G). GSK3β^{ADKO} mice exhibited no significant changes in serum leptin concentrations but showed increased serum adiponectin concentrations (Figure S3H and S3I). The insulin-sensitizing adipokine adiponectin appears to promote the healthy expansion of AT and plays a crucial role in protecting against insulin resistance, diabetes, and other metabolic disorders.[42,43] It has been demonstrated that in both human studies and rodent models, adiponectin serves as a key regulator of insulin sensitivity, energy expenditure, glucose and lipid metabolism, and cardiovascular homeostasis. Furthermore, chronic overexpression of adiponectin has also been observed to lead to a healthy extension of subcutaneous white adipose tissue (sWAT), which in turn contributes to protection against diet-induced insulin resistance.[44] This beneficial impact of the hormone is also evident in the enhancement of mitochondrial functions and capillary density of obese AT.[45,46] These actions are thought to underpin the diverse beneficial impacts of adiponectin in addressing a range of metabolic complications.

The elevation of adiponectin levels in obese ATs due to GSK3 deficiency may serve as one of the mechanisms to alleviate obesity-associated insulin resistance. Consistently, enhanced insulin sensitivity was observed in both male and female obese GSK3β^{ADKO} mice compared with control GSK3β$^{fl/fl}$ mice, as evidenced by improved responses to glucose and insulin challenges (Figure 2I and 2J; Figure S3J and S3K) and lower fasting serum insulin levels (Figure 2K; Figure S3L). Increased AKT/PKB (AKT serine-threonine kinase/protein kinase B) phosphorylation indicated improved insulin signaling in eWAT of obese mice (Figure 2L through 2N). The enhanced insulin supply in AT was suggested by increased tissue insulin levels in eWAT of obese mice, but not in the liver or muscle (Figure 2O).

Adipocyte-Specific GSK3β Deficiency Decreases AT Inflammation and Reduces Adipocyte Size

Chronic low-grade inflammation is closely linked to the development of obesity-induced metabolic disorders.[14,47] Adipocyte-specific GSK3β deficiency suppressed inflammation in obese AT, as evidenced by reduced crown-like structures (Figure 3A and 3B), decreased F4/80 levels (Figure 3C), and inflammatory marker gene expression (Figure 3D). We performed an RNA-seq assay using eWAT of obese GSK3β^{ADKO} mice compared with the control obese GSK3β$^{fl/fl}$ mice. Of the DEGs identified, 184 were upregulated and 479 were downregulated (P<0.05, log2 FC>log2(2); Figure S4A). Gene ontology analysis of downregulated DEGs in GSK3β^{ADKO} eWAT revealed enriched terms related to inflammation and inflammatory cytokine production (Figure 3E). A global downregulation of inflammation-associated genes was observed (Figure 3F). Kyoto Encyclopedia of Genes and Genomes enrichment analysis of the downregulated DEGs indicated that some enriched pathways related to inflammation and associated chemokine signaling in the eWAT of GSK3β^{ADKO} mice (Figure S4B), which was further confirmed by gene set enrichment analysis (Figure S4C through S4F).

UCP1 (uncoupling protein 1) levels did not increase in eWAT, sWAT, and brown AT as displayed by RT-PCR (Figure S4G through S4I) and UCP1 staining (Figure S4J), indicating that GSK3β deficiency in adipocytes has a limited impact on the thermogenic gene program. However, increased expression of *Pgc1α*, *Cox5b*, and *Cox8b* genes suggested elevated mitochondrial metabolic activity, which was further supported by enhanced oxidative phosphorylation (OxPhos)-associated gene expression at the mRNA level (Figure S4K) and OxPhos complexes at the protein level in eWAT with GSK3β ablation (Figure 3G). Both Kyoto Encyclopedia of Genes and Genomes and gene set enrichment analysis revealed that GSK3β^{ADKO} eWAT were positively associated with energy metabolic pathways, including OxPhos and insulin signaling (Figure S4L through S4N). We also compared 2 sets of DEGs. The first set was from a comparison between the eWAT of lean and obese GSK3$^{fl/fl}$ mice. Of the DEGs identified, 520 were upregulated and 1097 were downregulated (P<0.05, $\log_2$ FC>$\log_2$(2); Figure S4O). The second set was derived from a comparison between the eWAT from obese GSK3β^{ADKO} and obese GSK3$^{fl/fl}$ mice (Figure S4A). The comparison of these 2 sets of DEGs revealed 113 commonly upregulated genes and 430 co-downregulated genes (Figure S4P and S4Q). Inflammation-associated gene ontology terms were enriched among the co-downregulated DEGs of the lean and GSK3β^{ADKO} groups compared with control obese GSK3$^{fl/fl}$ mice, respectively (Figure S4R). Kyoto Encyclopedia of Genes and Genomes analysis identified metabolic pathways in

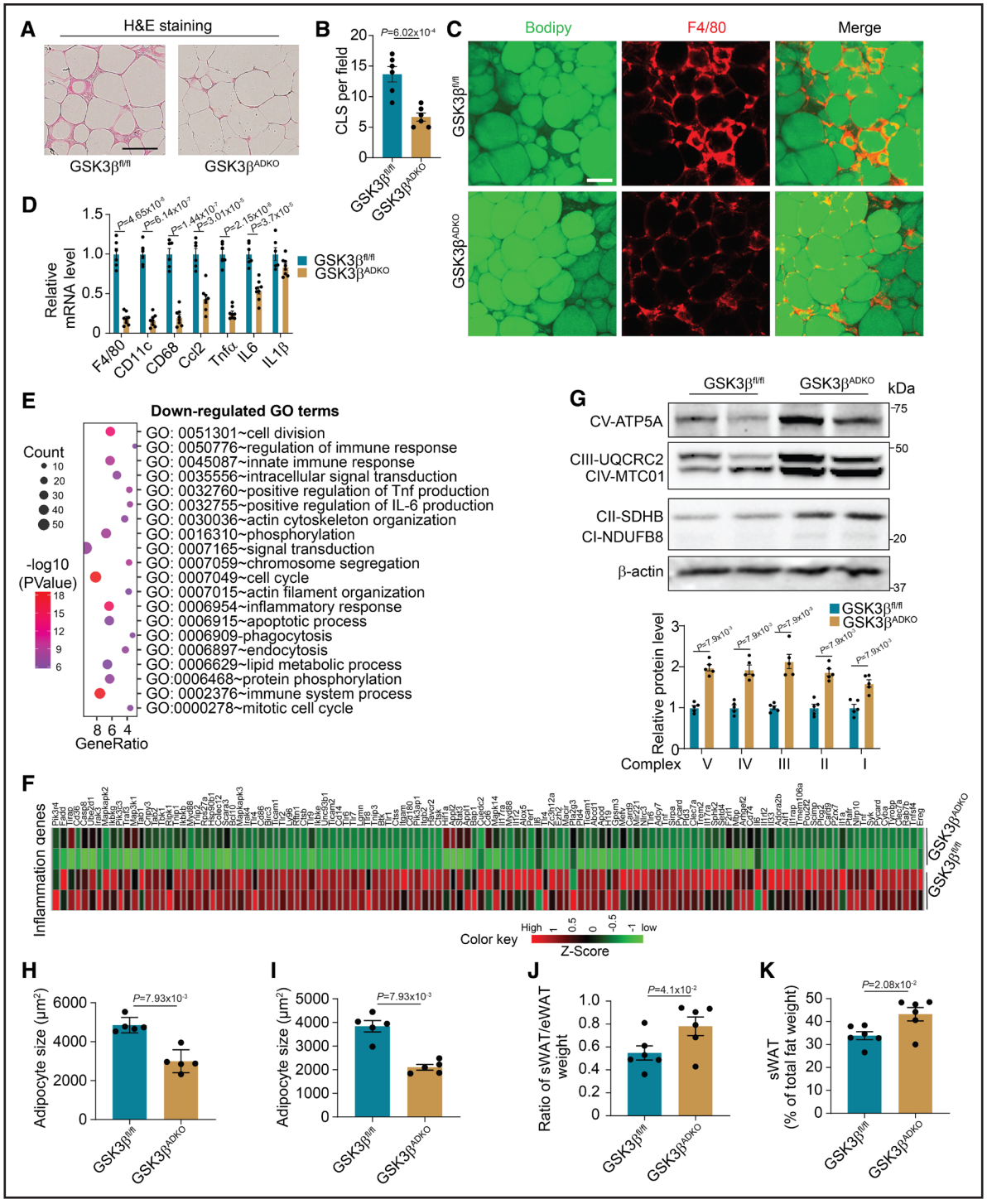

Figure 3. Adipocyte-specific GSK3β (glycogen synthase kinase-3 beta) deficiency reduces obesity-associated adipose tissue inflammation, increases OxPhos complexes, and decreases adipocyte size. Male GSK3β$^{fl/fl}$ and GSK3β^{ADKO} mice were fed a high-fat diet to induce obesity and used for the experiments.

A through **D**, Hematoxylin and eosin staining of epididymal white adipose tissue (eWAT; **A**), quantification of crown-like structures (CLS; **B**; n=6), and F4/80 staining (red) of eWAT sections (**C**). Lipids were stained green using BODIPY to indicate adipocytes (**C**), and the expression levels of inflammation-associated genes in eWAT were determined using reverse transcription polymerase chain reaction (**D**; n=6 for GSK3β$^{fl/fl}$ and n=8 for GSK3β^{ADKO}). **E**, Gene ontology (GO) term analysis of RNA sequencing data showing downregulated gene signatures in the eWAT of obese GSK3β^{ADKO} vs obese control GSK3β$^{fl/fl}$ mice. **F**, Heat map of expression values (*Z* score) for inflammation-associated genes in eWAT from the indicated obese mice. **G**, Western blotting images of oxidative phosphorylation (OxPhos) complexes and quantification using ImageJ software (n=5). **H** and **I**, Comparison of average adipocyte sizes measured as the adipocyte area of eWAT (**H**) and subcutaneous white adipose tissue (sWAT; **I**) from obese GSK3β$^{fl/fl}$ and GSK3β^{ADKO} mice (n=5). **J** and **K**, The ratio of sWAT to eWAT weight (**J**) and the percentage of sWAT weight in total fat weight (**K**) of male obese GSK3β$^{fl/fl}$ and GSK3β^{ADKO} mice (n=6). Scale bar=100 μm. **B**, **D**, **J**, and **K**, Two-tailed unpaired *t* test; **G** through **I**, nonparametric test.

co-upregulated DEGs (Figure S4S). These data support the idea that GSK3β ablation counters obese-specific gene expression patterning toward a lean-specific gene expression pattern.

Compared with control mice, GSK3β^{ADKO} mice displayed significantly smaller average adipocyte sizes in both eWAT and sWAT (Figure S3H and S3I), along with more uniform size and an increased adipocyte count per unit area in eWAT and, notably, in sWAT, as evidenced by the adipocyte area, its distribution, and the number of adipocytes in AT (Figure S5A through S5F). Reduced adipocyte size in GSK3β^{ADKO} mice suggests that GSK3β deficiency leads to AT remodeling, transitioning from AT hypertrophy (characterized by enlarged adipocytes) to hyperplasia (characterized by smaller adipocytes) during obesity. This shift decreases unhealthy expansion of AT, potentially improving the inflammatory microenvironment in tissues and preserving healthy adipocyte function. Visceral and subcutaneous obesity are linked with different risks of metabolic syndrome. Increased visceral fat distribution is associated with a high risk of metabolic disorders, whereas increased subcutaneous fat has beneficial effects on insulin sensitivity and metabolism.[48,49] We observed a significant increase in the sWAT-to-eWAT weight ratio in obese GSK3β^{ADKO} mice compared with control obese mice (Figure 3J) but not in lean mice (Figure S5G). We also noted a significant increase in the percentage of sWAT weight relative to the combined weight of sWAT and eWAT from obese mice (Figure 3K) but not lean mice (Figure S5H), implying the improved insulin response of obese GSK3β^{ADKO} mice is partially attributable to an increase in subcutaneous adipose depots.

Increased adipogenic potential, forming new adipocytes through adipogenesis (hyperplasia), is linked to a healthier expansion of WAT and reduced obesity-related proinflammatory effects and metabolic complications.[50,51] The vasculature is considered to support adipogenesis by serving as a niche where preadipocytes reside, undergo differentiation commitment, and mature into adipocytes.[13,52] The coordination of adipogenesis and angiogenesis is crucial for maintaining metabolic homeostasis. In obesity, the uncoupling of angiogenesis and adipogenesis leads to reduced vascularity, resulting in local hypoxia, oxidative stress, fibrosis, and other metabolic disorders within AT.[53] To evaluate whether adipogenic potential is affected in obese AT, we isolated SVF from both sWAT and eWAT of obese GSK3β^{ADKO} and control mice and performed in vitro adipocyte differentiation of adipocyte progenitor cells from these SVFs. We observed that SVF progenitor cells isolated from the sWAT of obese GSK3β^{ADKO} mice displayed higher lipid accumulation compared with SVF progenitor cells from the sWAT of control mice, as evidenced by both Oil Red O staining assay and mRNA levels of some general markers for adipocyte differentiation (Figure S5I and S5J). The differentiation of SVF progenitor cells from eWAT exhibited notably lower levels compared with SVF cells from sWAT (Figure S5I and S5K). While there was a rising trend in PPARγ (peroxisome proliferator-activated receptor gamma) expression and a notable increase in adiponectin mRNA levels observed in the in vitro-differentiated adipocytes of eWAT SVF progenitor cells, no significant variance in lipid accumulation was noted when inducing differentiation of eWAT SVF progenitor cells from obese GSK3β^{ADKO} mice compared with obese control mice. This was evidenced by comparable levels of Oil Red O staining in the cells (Figure S5K and S5L). These data suggest a discernible difference in the adipogenic potential between progenitor cells originating from sWAT and eWAT, partially elucidating the elevated sWAT/eWAT ratio observed in obese GSK3β^{ADKO} mice.

These findings also suggest that the slightly increased cell number in eWAT of obese GSK3β^{ADKO} mice may not be due to an enhanced adipogenic potential of eWAT progenitors. Adipocyte death increases in frequency during obesity and is more prevalent in eWAT compared with sWAT. Adipocyte death is an early and progressive event that triggers AT inflammation and complications associated with obesity.[54] We observed a downregulation in the expression levels of several genes associated with apoptosis, particularly those genes associated with inflammatory cell death, such as *Casp1*, *Aim2*, and *Pycard*, in the eWAT of obese GSK3β^{ADKO} mice compared with control mice (Figure S5M). While some apoptosis-associated genes were downregulated, this distinct pattern was not as prominently observed in the sWAT of obese GSK3β^{ADKO} mice (Figure S5N). These results suggest that the alteration in the number of adipocytes in eWAT may be attributed to a reduction in adipocyte death in obese GSK3β^{ADKO} mice rather than to the change of adipogenesis of progenitor cells.

Adipocyte-Specific GSK3β Deficiency Expanded the AT Vasculature

Both gene set enrichment analysis and gene ontology analysis of the upregulated DEGs in the eWAT of obese GSK3β^{ADKO} mice identified positively correlated pathways and enriched terms associated with angiogenesis and the response to hypoxia (Figure 4A; Figure S6A through S6D). These terms were also found among the co-upregulated DEGs from the lean control and obese GSK3β^{ADKO} groups compared with control obese GSK3β$^{fl/fl}$ mice (Figure S6E). The heat map demonstrated elevated mRNA levels of angiogenesis-associated genes (Figure 4B) and genes responsive to hypoxia in the obese eWAT of GSK3β^{ADKO} mice (Figure S6F). Furthermore, RT-PCR validation confirmed increased mRNA expression of angiogenesis marker genes (Figure 4C). Increased protein levels of VEGF, VEGFB, and VEGFR2, but not VEGFR1, were observed in the eWAT of obese GSK3β^{ADKO} mice (Figure 4D and

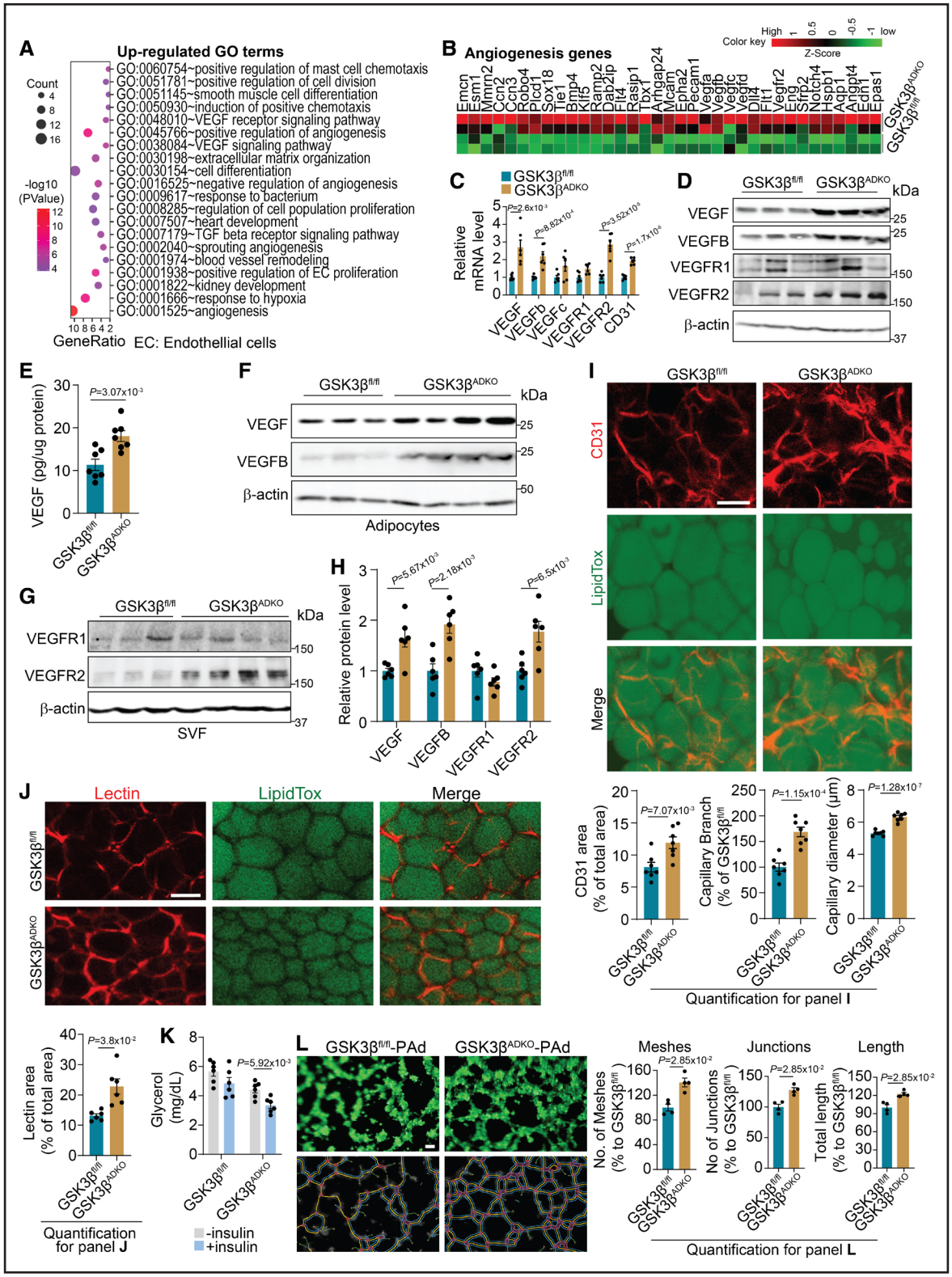

Figure 4. Ablation of GSK3β (glycogen synthase kinase-3 beta) in adipocytes stimulates the expansion of adipose tissue (AT) vasculature and upregulates the expression of genes associated with angiogenesis in the AT of obese mice.

Male C57Bl/6J GSK3βfl/fl and GSK3βADKO mice were fed a high-fat diet to induce obesity and used for the experiments. **A**, Gene ontology (GO) analysis showing upregulated gene signatures in the epididymal white adipose tissue (eWAT) of obese GSK3β^{ADKO} vs obese GSK3β$^{fl/fl}$ mice (n=2). **B**, Heat map of expression values (*Z* score) for angiogenesis-associated genes in eWAT from the indicated obese mice. **C**, Validation of angiogenesis-associated genes using reverse transcription polymerase chain reaction (n=6). **D**, Western blotting analysis of the indicated proteins in eWAT from the indicated obese mice. **E**, VEGF (vascular endothelial growth factor) protein level analysis using ELISA in eWAT (*Continued*)

4E; Figure S6G). Increased VEGF and VEGFB proteins mainly originate from adipocytes, whereas increased VEGFR2 protein is derived from the SVF component (Figure 4F through 4H). VEGFB activates the VEGF/VEGFR2 pathway by displacing VEGF from its binding with VEGFR1, resulting in the subsequent binding of VEGF to VEGFR2. This process remodels the vascular structure and enhances insulin signaling in AT.[16,55–57] This partially explains why GSK3β^{ADKO} mice displayed increased levels of both VEGF and VEGFB in adipocytes. Furthermore, whole-mount staining demonstrated higher CD31 expression, as well as increased vessel size and expanded capillary network in eWAT of obese GSK3β^{ADKO} mice compared with control mice (Figure 4I). Increased expression of angiogenesis marker genes and an expanded AT capillary network were also detected in the sWAT and brown AT of GSK3β^{ADKO} mice (Figure S6H through S6K). These data imply that GSK3β deficiency regulates angiogenesis to modulate the vascular network within obese AT. GSK3β^{ADKO} mice also displayed increased vessel perfusion in eWAT, as indicated by the increased presence of lectin-perfused areas (Figure 4J), partially explaining the observation that AT showed an increased insulin supply and increased insulin signaling. Consistently, the obese GSK3β^{ADKO} mice also exhibited reduced serum glycerol concentrations after the injection of insulin compared with the GSK3β$^{fl/fl}$ control mice, suggesting inhibited lipolysis by insulin and retained insulin sensitivity at the tissue level (Figure 4K).

Intriguingly, in our in vitro co-culture experiments, we observed that when primary mature adipocytes isolated from obese GSK3β^{ADKO} mice were cocultured with endothelial 3B-11 or mouse hemangioendothelioma endothelial cells, there was a notable enhancement in the angiogenic potential of the endothelial cells. This was evidenced by a significant increase in tube formation compared with cocultures with obese GSK3β$^{fl/fl}$ primary adipocytes (Figure 4L; Figure S7A through S7D). When culturing 3B-11 cells in conditional medium obtained from GSK3β inhibitor-treated mature 3T3-L1 adipocytes under hypoxia (1% O_2) to mimic the hypoxic environment in obese AT, we also observed enhanced tube-formation capability compared with cells cultured in the control conditional medium (Figure S7E through S7H). VEGF secretion was enhanced in the conditional medium from adipocytes cultured with a GSK3 inhibitor under hypoxia for 24 hours (Figure S7I).

We next used obese mice with adipocyte-specific GSK3α deletion to assess the role of GSK3α in AT vasculature. Heat map analysis from RNA-seq data revealed no differences in the expression of angiogenesis-associated genes between the GSK3α^{ADKO} and control GSK3α$^{fl/fl}$ groups (Figure S7J), implying a clear difference between GSK3β and GSK3α in regulating AT vasculature. This result was further validated by RT-PCR results, which showed no significant changes in angiogenesis-associated gene expression in the eWAT of GSK3α^{ADKO} mice compared with control mice (Figure S7K). These data suggest that the adipocyte-specific functions of GSK3β, but not GSK3α, affect the vasculature in AT, likely by mediating communication between adipocytes and endothelial cells, which may be mediated by the release of VEGF from adipocytes to act on endothelial cells.

Adipocyte-Specific GSK3β Deficiency Counteracts the Deteriorated Microenvironment in Obese AT

Emerging studies have shown that induced vascularization has beneficial effects on pathological changes during obesity.[13,15,16,24] We evaluated the hypoxia status of AT and observed low pimonidazole hypoxyprobe staining, indicating less hypoxia in the eWAT and sWAT of GSK3β^{ADKO} mice than GSK3β$^{fl/fl}$ control mice (Figure 5A; Figure S8A and S8B). Reduced hypoxia levels imply a greater oxygen supply to the tissues; therefore, we measured the oxygen consumption rate of AT. The results showed that, compared with the eWAT of obese GSK3β$^{fl/fl}$ mice, the eWAT of obese GSK3β^{ADKO} mice had significantly higher basal and maximal oxygen consumption rates for mitochondrial respiration (Figure 5B and 5C), as well as significantly higher oxygen consumption rates for ATP production (Figure 5D), suggesting increased OxPhos capacity. These findings are consistent with upregulated expression of OxPhos-associated genes, as demonstrated by the RNA-seq data, and increased OxPhos complex protein (Figure 3G; Figure S4K). In contrast, a slight decrease was observed in the extracellular acidification rate (an indicator of anaerobic glycolysis) of the eWAT of GSK3β^{ADKO} mice (Figure S8C). The level of the insulin-dependent glucose transporter GLUT4 was found to be upregulated, whereas the level of GLUT1, an insulin-independent transporter induced by hypoxia

Figure 4 Continued. lysates from the indicated obese mice (n=7). **F** through **H**, Western blotting images of the indicated proteins in adipocytes (**F**) and stromal vascular fraction (SVF; **G**) from the indicated obese mice, along with their protein quantification (**H**; n=6). **I**, Representative images of whole-mount staining of eWAT for CD31 and analysis for CD31-positive area, capillary branch density, and capillary diameter quantified using Image J software (n=7). **J**, Representative images of whole-mount staining of eWAT from obese mice injected with lectin and quantification of the lectin area (n=6). **K**, Serum glycerol levels in the indicated obese mice before or 30 minutes after injection with 0.75 U/kg insulin (n=6). **L**, In vitro tube-formation assay of 3B-11 mouse endothelial cells cocultured with primary adipocytes (Pad, passage 0 [P0]) isolated from the indicated obese mice. Analysis is for the number of meshes, number of junctions, and total segment length (n=4). Scale bar=100 μm. **C**, **E**, and **H** through **K**, Two-tailed unpaired *t* test; **L**, nonparametric test.

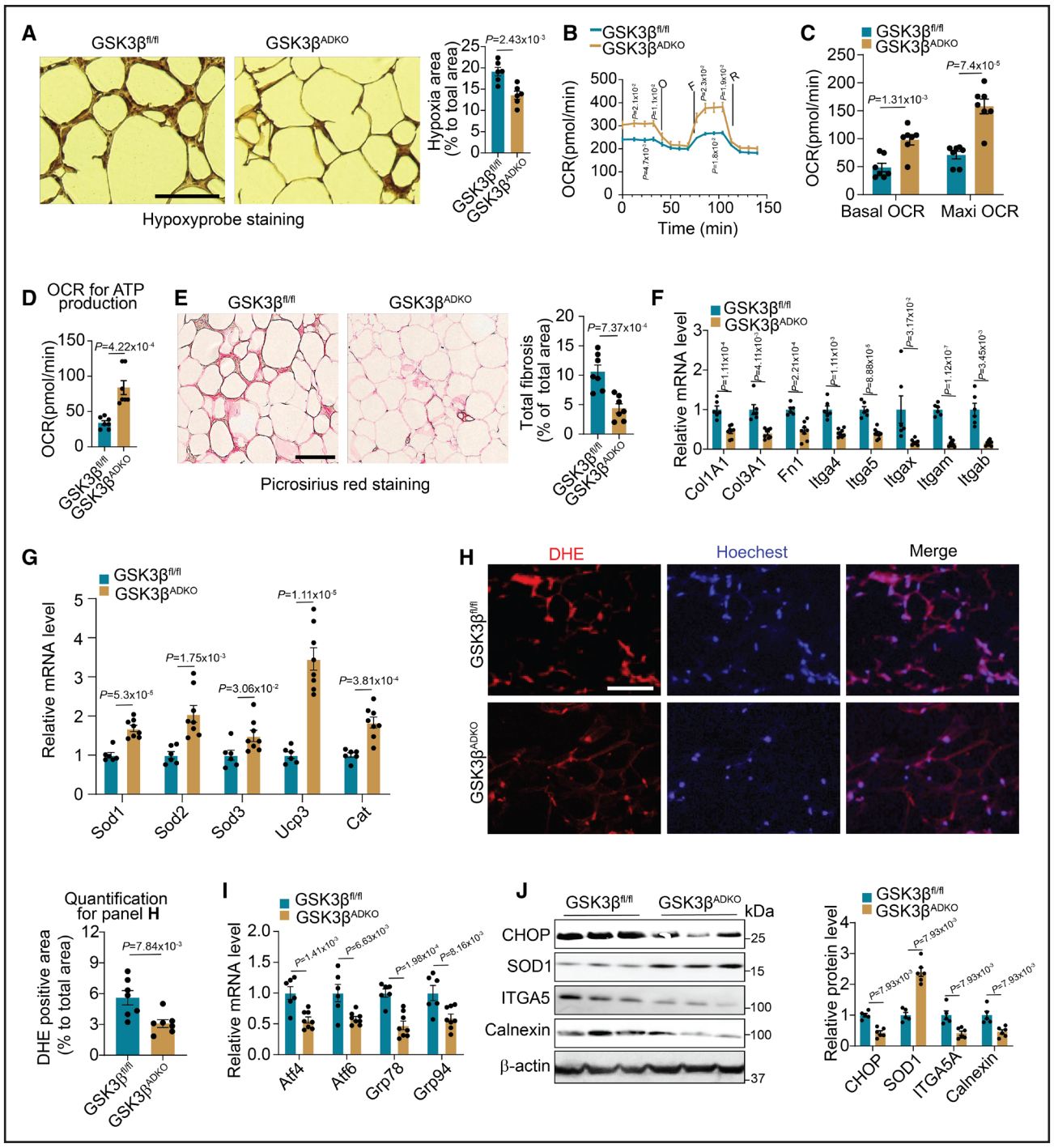

Figure 5. Adipocyte-specific GSK3β (glycogen synthase kinase-3 beta) deficiency reduces hypoxia, fibrosis, and reactive oxygen species (ROS) levels in obese adipose tissue, leading to an improved microenvironment.

Male GSK3β$^{fl/fl}$ and GSK3β^{ADKO} mice were fed a high-fat diet to induce obesity and used for the experiments. **A**, Representative images of hypoxyprobe staining of epididymal white adipose tissue (eWAT) and quantification of staining from the indicated obese mice (n=6). **B** through **D**, Total oxygen consumption rates (OCRs; **B**), basal OCRs and OCRs for maximal (Maxi) respiratory capacity (**C**), and OCRs for ATP production (**D**) of eWAT from the indicated obese mice (n=7). **E**, Representative images of picrosirius red staining (detecting collagen for fibrosis analysis) and its quantification for fibrosis analysis of eWAT from the indicated obese mice (n=7). **F** through **G**, Fibrosis- (**F**; n=6 for GSK3β$^{fl/fl}$ and n=8 for GSK3β^{ADKO}) and antioxidative stress- (**G**; n=6) associated gene expression analysis performed using reverse transcription polymerase chain reaction (RT-PCR). **H**, ROS staining (dihydroethidine [DHE] dye) of eWAT sections from the indicated obese mice and quantification using ImageJ software (n=7). **I**, Expression analysis of ER stress-associated genes performed using RT-PCR (n=6 for GSK3β$^{fl/fl}$ and n=8 for GSK3β^{ADKO}). **J**, Western blotting analysis of the indicated proteins and quantification using ImageJ software in eWAT of indicated obese mice (n=5 for GSK3β$^{fl/fl}$ and n=6 for GSK3β^{ADKO}). Scale bar=100 μm. O: oligomycin; F: FCCP; R: Rot/AA. **A**, **C** through **I**, Two-tailed unpaired *t* test; **B**, repeated ANOVA and Bonferroni post hoc test; **J**, nonparametric test.

ORIGINAL RESEARCH

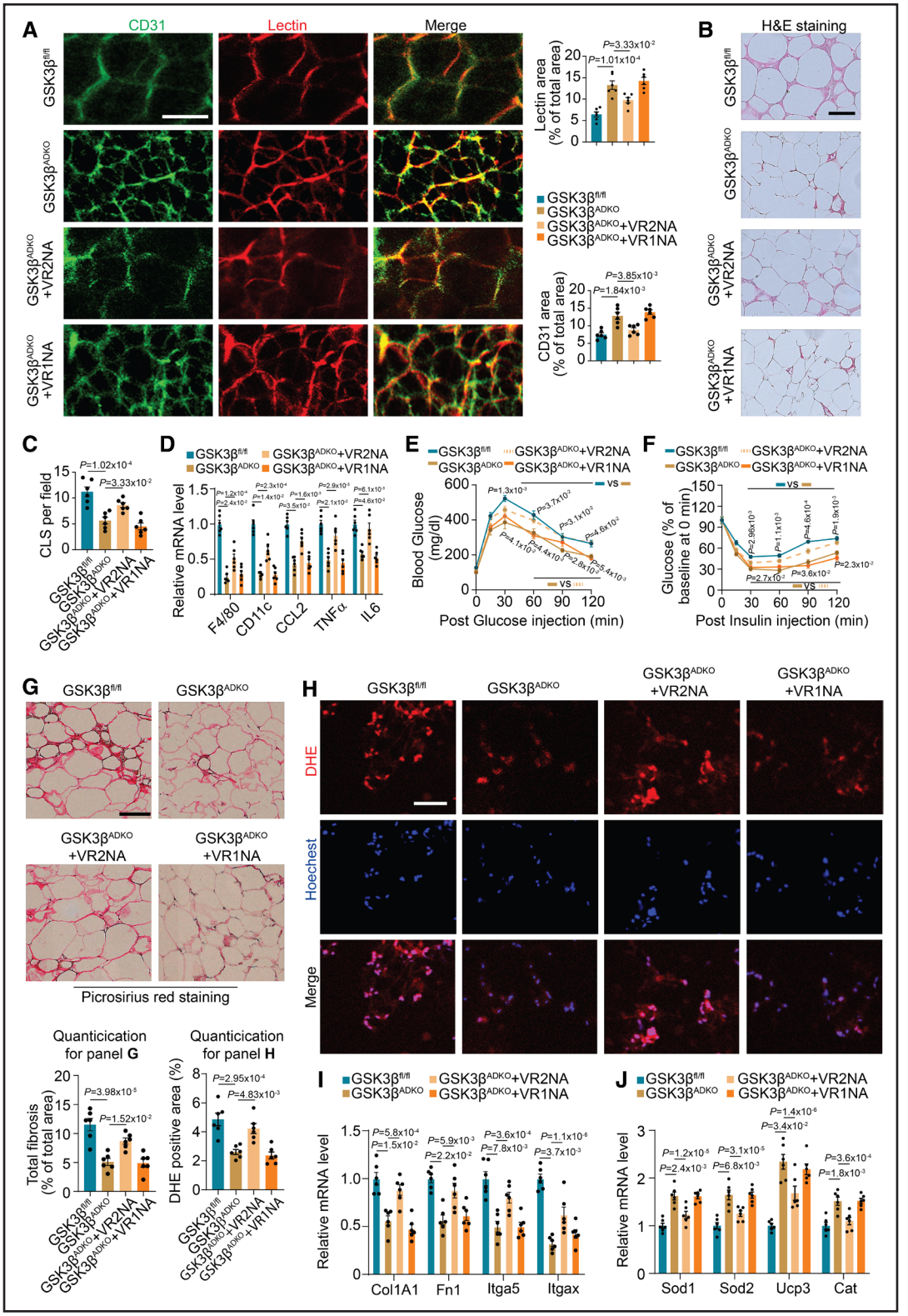

Figure 6. VEGFR2 mediates the improvement of vascularity, metabolic complications, and the tissue microenvironment in obese adipose tissue resulting from adipocyte-specific ablation of GSK3β (glycogen synthase kinase-3 beta).
Male GSK3β$^{fl/fl}$ and GSK3β^{ADKO} mice were fed a high-fat diet to induce obesity. The induced obese GSK3β^{ADKO} mice were then treated with either IgG or VEGFR1- (GSK3β^{ADKO}+VR1NA) or VEGFR2-neutralizing antibodies (GSK3β^{ADKO}+VR2NA) for use in the experiments. **A**, Representative image of epididymal white adipose tissue (eWAT) whole-mount staining of lectin and CD31 from the indicated obese mice injected with lectin and quantification of the lectin-perfused area and CD31-positive area (n=6). **B** and **C**, Hematoxylin and eosin staining of eWAT (**B**) and crown-like structure [CLS] quantification (**C**) in the indicated obese mice (n=6) using ImageJ software. **D**, The expression of inflammation (*Continued*)

in fat cells,[10,58] was downregulated in the eWAT of obese GSK3β^{ADKO} mice (Figure S8D), suggesting a shift from anaerobic respiration to aerobic respiration. Furthermore, obesity-induced AT fibrosis was found to be alleviated in GSK3β^{ADKO} mice, as shown using collagen deposition analysis (picrosirius red staining for collagens I and III; Figure 5E). This finding is supported by the RNA-seq data, which showed decreased fibrosis-associated gene expression (Figure S8E), as well as the RT-PCR validation (Figure 5F). In addition, GSK3β ablation increased antioxidant gene expression and decreased ROS-associated gene expression (Figure 5G; Figure S8F). Diminished intensity of dihydroethidine staining was consistent with lower production of superoxide in the eWAT of obese GSK3β^{ADKO} mice than GSK3β$^{fl/fl}$ mice (Figure 5H). The eWAT of obese GSK3β^{ADKO} mice exhibited lower mRNA levels of ER stress marker genes, such as *Atf4/6* and *GRP78/94* (also known as *Hspa5/Hsp90b1*), than the GSK3β$^{fl/fl}$ mice as well (Figure 5I), in line with the RNA-seq data as revealed in the heat map (Figure S8G). The levels of ER stress markers, such as CHOP and calnexin, and the fibrosis marker ITGA5 were all downregulated at the protein level, but the antioxidant marker SOD1 was increased in the eWAT of obese GSK3β^{ADKO} mice (Figure 5J). Less pimonidazole staining was also observed in obese mice treated with GSK3 inhibition (Figure S8H). Consistently, the expression of fibrosis-associated genes was downregulated (Figure S8I), but the expression of antioxidant genes such as *Sod1*, *Cat*, and *Ucp3* was upregulated while the expression of ROS generation-associated genes such as *Ncf2* was downregulated in the eWAT of obese mice with GSK3 inhibition (Figure S8J). Together, these data indicate that GSK3β deletion expanded the AT vasculature to improve obesity-induced microenvironment deterioration, leading to improved metabolic homeostasis.

VEGFR2 Is Required for Vascular Remodeling in Obese AT Caused by GSK3β Deficiency in Adipocytes

We observed that upon GSK3β knockout in AT, both VEGF and VEGFB derived from the adipocytes increased significantly, whereas VEGFR2 showed a significant increase in the SVF component of AT. We hypothesized that GSK3β deficiency in adipocytes increased VEGFB, which stimulates VEGF to bind to VEGFR2, expressed in endothelial cells of SVF from AT to activate the VEGF/VEGFR2 signaling pathway. To test this hypothesis, we injected VEGFR1- and VEGFR2-neutralizing antibodies into obese mice. We observed the abolished expansion of capillary density induced by GSK3β deficiency, characterized by limited lectin-perfused and CD31-positive areas in AT after VEGFR2-neutralizing antibody treatment (Figure 6A). By contrast, anti-VEGFR1 antibody treatment did not significantly affect vasculature expansion (Figure 6A). The GSK3β-deficiency-induced reduction in inflammation in AT was reversed by anti-VEGFR2 antibody treatment, as indicated by an increased number of crown-like structures surrounding the adipocytes and the results of the inflammation-associated gene expression analysis (Figure 6B through 6D). The VEGFR2-neutralizing antibody also reversed the beneficial effects caused by GSK3β deletion on glucose tolerance and insulin sensitivity (Figure 6E and 6F). Moreover, VEGFR2-neutralizing antibody treatment resulted in increased fibrosis, as indicated by picrosirius red staining (Figure 6G), and increased ROS production, as shown by dihydroethidine staining (Figure 6H), in the eWAT of obese GSK3β^{ADKO} mice, as compared with vehicle treatment. Similarly, fibrosis-associated genes showed increased expression (Figure 6I), but antioxidant genes showed decreased expression upon anti-VEGFR2 antibody treatment (Figure 6J). Taken together, these data are consistent with the idea that adipocyte-specific GSK3β deficiency activates the VEGF/VEGFR2 signaling pathway, which mediates crosstalk between adipocytes and the surrounding endothelial cells and results in increased vasculature and prevents tissue dysfunction in obese mice.

HIF-2α Mediates the Effects of GSK3β Ablation on Increased AT Vasculature and the Improved Microenvironment

HIF-1α mRNA was increased, whereas HIF-2α mRNA was decreased, in obese eWAT compared with lean eWAT, but no change was observed for HIF-1β mRNA (Figure S9A). HIF-2α was significantly increased at both the mRNA (Figure S9B) and protein levels in eWAT of the obese GSK3β^{ADKO} mice in comparison to GSK3β$^{fl/fl}$ mice (Figure 7A and 7B; Figure S9C). In contrast, HIF-1α expression showed marginal change (Figure 7A and 7B; Figure S9C), despite downregulation of HIF-1α target genes (Figure S9D). Consistently,

Figure 6 Continued. marker genes in eWAT was determined using reverse transcription polymerase chain reaction (RT-PCR; n=6). **E** and **F**, Glucose tolerance test (**E**) and insulin tolerance test (**F**) in the indicated mice (n=6). **G**, Representative picrosirius red staining and its quantification for fibrosis analysis of eWAT in the indicated mice (n=6). **H**, Reactive oxygen species staining (dihydroethidine [DHE] dye) of eWAT sections from the indicated mice and quantification using ImageJ software (n=6). **I** and **J**, Expression analysis using RT-PCR for fibrosis-associated genes (**I**) and antioxidative stress-associated genes (**J**; n=6). Scale bar=100 μm. **A**, **C**, **D**, and **G** through **I**, One-way ANOVA and Tukey post hoc test; **E** and **F**, repeated ANOVA and Bonferroni post hoc test. VR1NA indicates VEGFR1-neutralizing antibody; and VR2NA, VEGFR2-neutralizing antibody.

ORIGINAL RESEARCH

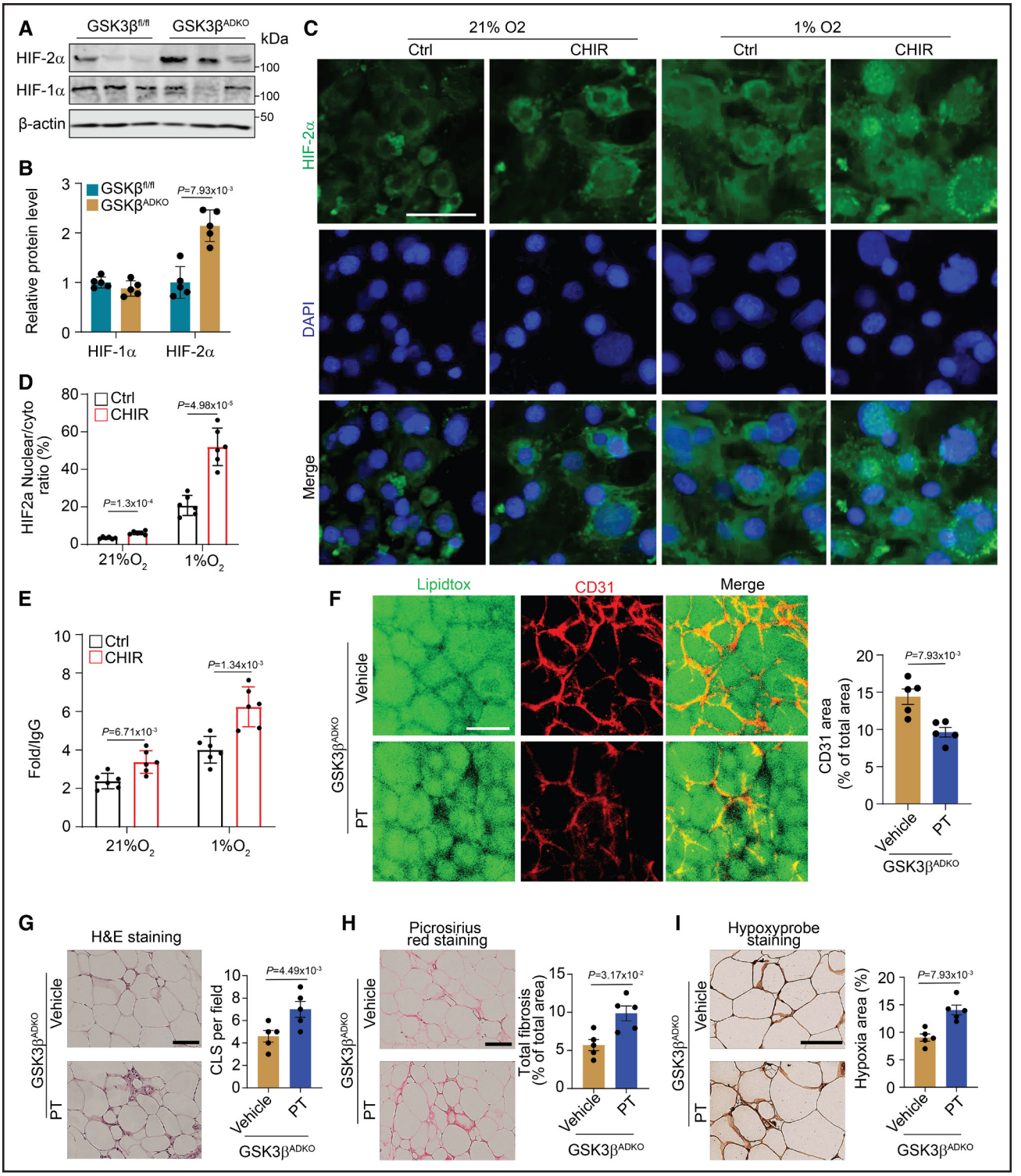

Figure 7. The effects of adipocyte-specific GSK3β (glycogen synthase kinase-3 beta) ablation on expanded tissue vascularity and improved microenvironment of obese adipose tissue are mediated by HIF-2α (hypoxia-inducible factor 2-alpha).
Male GSK3β$^{fl/fl}$ and GSK3β^{ADKO} mice were fed a high-fat diet to induce obesity. The induced obese GSK3β^{ADKO} mice were then treated with or without the HIF-2α inhibitor PT2385 (GSK3β^{ADKO}+PT [30 mg/kg]) for 2 weeks for use in the experiments of **A** and **B**, and **F** through **I**. **A** and **B**, Expression analysis of HIF-1α and HIF-2α at the protein level using Western blotting (**A**) in epididymal white adipose tissue (eWAT) of indicated obese mice and quantification using ImageJ software (**B**; n=5). **C**, Nuclear accumulation of HIF-2α in mature 3T3-L1 adipocytes, with or without GSK3 inhibitor CHIR99021 (CHIR, 10 μmol/L) treatment, under hypoxic (1%) and normoxia (21%) conditions for 4 hours. The nuclei were visualized using 4′,6-diamidino-2-phenylindole (DAPI) staining. **D**, Analysis of HIF-2α nuclear/cytoplasmic ratio from the experiments presented in **C** (n=6). **E**, Chromatin immunoprecipitation (ChIP) analysis of HIF-2α at the *VEGF*-hypoxia response element after 4 hours of 1% O_2 treatment with GSK3 inhibition (n=5). **F**, Whole-mount CD31 staining and CD31-positive area quantification of eWAT sections from the (*Continued*)

HIF-2α target genes were upregulated (Figure S9E). Our data showed that VEGF was also upregulated in the eWAT of obese GSK3β^{ADKO} mice, consistent with the HIF-2α upregulation. Considering that both HIF-1α and HIF-2α function as transcription factors by translocating into the nucleus to regulate VEGF expression,[59] we utilized in vitro-differentiated 3T3-L1 adipocytes to evaluate the expression and translocation of HIF-1α and HIF-2α upon GSK3β inhibition. Under normoxia conditions, the HIF-1α expression was low, and GSK3 inhibition did not alter the expression or the subcellular localization of HIF-1α (Figure S9F and S9G). Meanwhile, hypoxic culture conditions significantly increased both protein levels and nuclear accumulation of HIF-1α (Figure S9F and S9G), whereas GSK3 inhibition blocked its nuclear accumulation (Figure S9F and S9G). Nuclear accumulation of HIF-2α was stimulated by hypoxia, and this was further increased by the treatment of GSK3 inhibitor, CHIR99021 (CHIR) treatment (Figure 7C and 7D). Chromatin immunoprecipitation assays showed increased binding of HIF-2α to the *VEGF*-hypoxia response element after 4 hours at 1% O_2 with GSK3 inhibition (Figure 7E). Additionally, slight binding of HIF-2α to the *VEGF*-hypoxia response element was noted under normoxia conditions upon GSK3 inhibition (Figure 7E). ELISA assays revealed a notable elevation in VEGF levels in the culture medium of GSK3 inhibitor-treated 3T3-L1 cells compared with control cells. This increase became more pronounced after 24 hours of exposure to hypoxic conditions (Figure S9H). The results indicate that inhibition of GSK3 may enhance the nuclear accumulation of HIF-2α, thereby increasing its transcriptional regulatory activity. Conversely, GSK3 inhibition suppresses the nuclear accumulation of HIF-1α and its transcriptional regulatory activity.

Furthermore, we utilized PT2385, an HIF-2α-specific inhibitor that effectively suppresses the expression of HIF-2α target genes by allosterically disrupting the HIF-2α/ARNT heterodimerization.[60] We administered this inhibitor to obese GSK3β^{ADKO} mice to assess its impact on tissue vascularity and the corresponding microenvironment. Our results showed that HIF-2α inhibition blocked vasculature expansion induced by GSK3β^{ADKO} in both male and female obese AT (Figure 7F; Figure S9I and S9J). The HIF-2α inhibitor diminished the beneficial effects of GSK3β^{ADKO} on inflammation as indicated by the increased crown-like structure area (Figure 7G) and upregulated inflammatory marker levels (Figure S9K and S9L). Fibrosis and hypoxia were also intensified, as evidenced by stronger picrosirius red staining (Figure 7H) and hypoxyprobe staining (Figure 7I; Figure S9M and S9N), respectively. Taken together, these data strongly suggest that the HIF-2/VEGF axis functions as a downstream target of GSK3β in the regulation of AT vasculature.

AMPK Mediates the Effects of GSK3β Ablation on the HIF-2/VEGF Axis

To address whether any molecules act as effectors to mediate the abovementioned effects on HIF-2α translocation upon GSK3 inhibition, we performed a multiplex immunoassay using protein extracts of the eWAT of GSK3β$^{fl/fl}$ control and GSK3β^{ADKO} mice. A significant increase was detected in the phosphorylation of some kinases such as AKT/PKB, mammalian target of rapamycin, and ERK (extracellular signal-regulated kinase; Figure S10A and S10B). Nuclear accumulation of HIF-2α appeared to be unaffected in AKT/PKB- or ERK inhibitor-treated 3T3-L1 adipocytes with GSK3 inhibition (Figure 8A and 8B). Interestingly, an AMPK inhibitor significantly blocked the GSK3 inhibition-induced nuclear accumulation of HIF-2α (Figure 8A and 8B). Moreover, we observed enhanced nuclear accumulation of HIF-1α in cells with AKT or AMPK inhibitor treatment (Figure S10C and S10D). AMPK inhibition also attenuated the increase in VEGF mRNA and protein levels (Figure S10E and S10F). Previous studies have shown that HIF-2α phosphorylation may mediate its activation and nuclear translocation.[61,62] Our findings demonstrated an increase in HIF-2α phosphorylation in adipocytes upon GSK3 inhibition, whereas the AMPK inhibitor mitigated this effect (Figure 8C). Additionally, we observed increased HIF-2α phosphorylation in obese eWAT when GSK3β was ablated, and the administration of an AMPK inhibitor reduced this increase (Figure 8D). HIF-1α phosphorylation remained unaffected in adipocytes treated with a GSK3β inhibitor. However, a slight increase in HIF-1α phosphorylation was observed in adipocytes treated with both GSK3 and AKT/PKB inhibitors, whereas no such effects were observed upon AMPK inhibitor treatment (Figure S10G and S10H). Taken together, our data indicate that AMPK may serve as a potential downstream mediator of the effects of GSK3β deficiency and may be responsible for regulating the nuclear accumulation of HIF-2α, as well as its transcriptional regulatory activity on target genes, possibly by modulating HIF-2α phosphorylation.

We further investigated the impact of GSK3β on AMPK activity. In 3T3-L1 adipocytes, we observed an increase in AMPK phosphorylation upon GSK3 inhibition

Figure 7 Continued. indicated obese mice (n=5). **G**, Hematoxylin and eosin staining of eWAT and CLS quantification in the indicated obese mice (n=5) using ImageJ software. **H**, Representative picrosirius red staining and quantification for the fibrosis analysis of eWAT from the indicated obese mice (n=5). **I**, Representative images of hypoxyprobe staining of eWAT and quantification of staining in the indicated mice (n=5). Scale bar=100 μm. **B** through **E**, Two-tailed unpaired *t* test; **F** through **I**, nonparametric test.

ORIGINAL RESEARCH

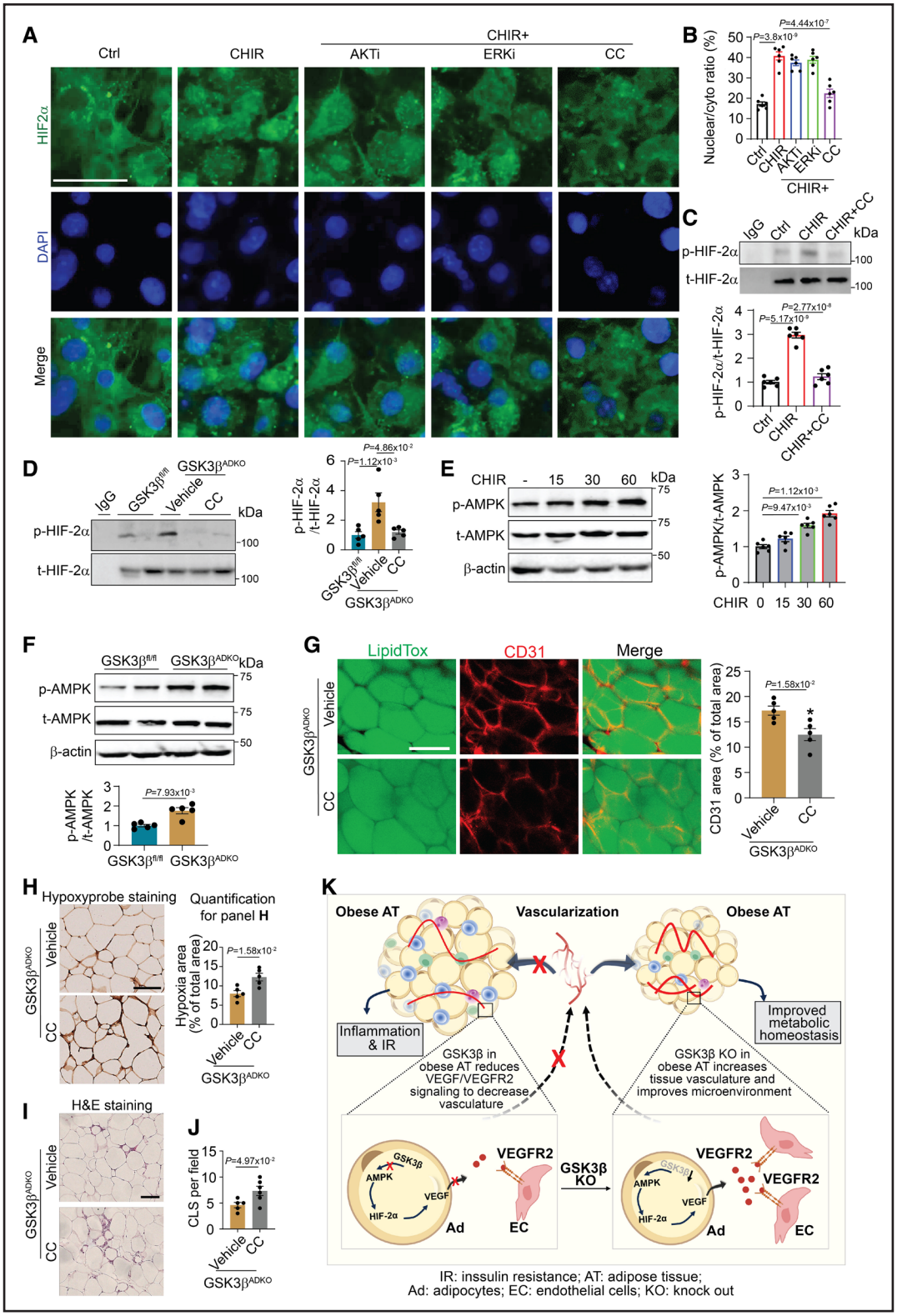

Figure 8. AMPK (AMP-activated protein kinase) regulates the HIF-2α/VEGF (hypoxia-inducible factor 2-alpha/vascular endothelial growth factor) axis to mediate the effects of adipocyte-specific GSK3β (glycogen synthase kinase-3 beta) deficiency on tissue vascularity and the microenvironment of obese adipose tissue by stimulating HIF-2α nuclear accumulation.
A and **B**, Nuclear accumulation of HIF-2α in mature 3T3-L1 adipocytes upon GSK3 inhibition with CHIR99021 (CHIR, 10 μM) and with or without the treatment of inhibitors targeting other kinases, AKT inhibitor-Triciribine (AKTi, 10 μmol/L), ERK inhibitor SCH772984 (ERKi, 300 nmol/L), and AMPK inhibitor (CC, 10 μmol/L) under hypoxic conditions (1%; **A**) for 4 hours. Analysis of nuclear/cytoplasmic ratios (**B**; n=6). **C** and **D**, HIF-2α phosphorylation analysis of pulled down total HIF-2α and quantification vs total HIF-2α in mature 3T3-L1 (*Continued*)

(Figure 8E). Similarly, elevated AMPK phosphorylation was detected in AT of obese GSK3β^{ADKO} mice compared with the eWAT of obese GSK3β$^{fl/fl}$ control mice (Figure 8F). These findings suggest that GSK3β negatively regulates AMPK activity in adipocytes and in the eWAT of obese mice. An AMPK inhibitor abated expansion of adipose vascularity caused by GSK3β deficiency, as evidenced by low levels of CD31 staining (Figure 8G; Figure S11A). AMPK inhibition also attenuated the beneficial effects of GSK3β^{ADKO} on hypoxia (Figure 8H; Figure S11B), fibrosis (Figure S11C), and inflammation, as indicated by the increased number of crown-like structures and inflammatory gene expression levels (Figure 8I and 8J; Figure S11D and S11E). Taken together, these findings suggest that GSK3β negatively affects the AMPK/HIF-2α axis, leading to the downregulation of VEGF/VEGFR2 activity in obese AT. Consequently, this impairs the vascularity of obese AT and results in a deteriorated microenvironment and increased inflammation (Figure 8K).

DISCUSSION

In our study, adipocyte-specific GSK3β deficiency was found to counteract obesity-related metabolic disorders and restore metabolic health in obese AT. These data underscore the role of GSK3β in remodeling the AT vasculature during obesity, which is achieved through the GSK3β/AMPK/HIF-2α/VEGF/VEGFR2 pathway, thus fostering crosstalk between adipocytes and endothelial cells. This process modulates the microenvironment in obese AT by stimulating angiogenesis, expanding the vasculature, and enhancing AT perfusion. Consequently, these changes ameliorate hypoxia, reduce ROS generation, alleviate ER stress, mitigate fibrosis, and reduce inflammation, ultimately improving insulin resistance. Our study is the first to report on the involvement of GSK3β in AT vascular remodeling during obesity, shedding light on its pathophysiological role in obesity-associated metabolic complications.

The functions of GSK3α and GSK3β vary across different tissues. However, the clinical application of GSK3 inhibitors is hindered by side effects, and further exploration is needed to understand their precise functions. It is, therefore, crucial to understand the roles of GSK3 isoforms in different tissues. Our study provides the first evidence that adipocyte-specific GSK3β deletion remodels AT vasculature, thereby regulating the microenvironment and metabolic activity. In contrast, GSK3α does not produce a similar impact on AT vasculature. Compared with visceral fat, subcutaneous fat has beneficial effects on glucose metabolism and insulin sensitivity.[48,49] We observed an increase in the amount of subcutaneous fat and in the sWAT/eWAT ratio in the presence of GSK3β deficiency, suggesting a shift toward peripheral obesity from central obesity.

It remains to be determined how AT growth is coordinated with capillary network expansion and what triggers AT vascularization during development and in obesity. Some reports demonstrated that the growth and functions of AT are highly reliant on the vasculature, primarily through angiogenesis, which not only supplies nutrients to adipocytes but also serves as a niche for adipocyte precursors.[15,52,53] Dysregulated angiogenesis or deficient AT angiogenesis can disrupt AT function and increase the risk of metabolic disorders in individuals with obesity, whereas modulated vascular patterns can impact the size and expandability of various adipose depots,[15,16,24,53] particularly the hypertrophic process characterized by an increase in cell size. Hypertrophic obesity is more closely associated with metabolic complications than hyperplastic obesity.[63,64] A simple and commonly accepted model suggests that the unhealthy expansion of WAT primarily occurs through adipocyte hypertrophy rather than hyperplasia, stemming from dysfunctional adipocyte progenitor cells.[51,65] This expansion, combined with inadequate angiogenesis, leads to overwhelmed and unhealthy adipocytes, resulting in hypoxia, cell death, and the subsequent activation of inflammation and fibrosis alongside metabolic disorders.[65] Collaborative interactions among adipocytes and various cell types within the AT microenvironment, including endothelial cells, immune cells, and adipocyte progenitor cells, have the potential to influence AT remodeling and contribute to maintaining tissue health and systemic metabolic homeostasis in obese mice.[66]

Our findings indicate that GSK3β deficiency reduces adipocyte size in AT and increases adipocyte number rather than promoting the enlargement of individual adipocytes. Furthermore, GSK3β deficiency stimulates adipocytes to release the angiogenic factor VEGF and the insulin-sensitizing hormone adiponectin. Adiponectin is

Figure 8 Continued. adipocytes with the indicated treatment for 4 hours (**C**, n=6) and in epididymal white adipose tissue (eWAT) from male GSK3β$^{fl/fl}$ and GSK3β^{ADKO} mice fed an high-fat diet treated with or without the AMPK inhibitor (GSK3β^{ADKO}+CC [10 mg/kg]) for 2 weeks (**D**, n=5). **E** and **F**, AMPK phosphorylation analysis in mature 3T3-L1 adipocytes with CHIR treatment (10 μmol/L) for indicated time points (**E**, n=6) and in eWAT from male obese GSK3β^{ADKO} and GSK3β^{ADKO}+CC mice (**F**, n=5). **G**, Whole-mount CD31 staining and CD31-positive area quantification from male obese GSK3β^{ADKO} and GSK3β^{ADKO}+CC mice (n=5). **H** through **J**, Representative images of hypoxyprobe staining of eWAT and quantification of staining (**H**, n=5), hematoxylin and eosin staining of eWAT (**I**) and CLS quantification (**J**, n=5) from male obese GSK3β^{ADKO} and GSK3β^{ADKO}+CC mice. **K**, A simplified scheme to represent how GSK3β regulates adipose tissue vasculature of obese mice. The absence of GSK3β in adipocytes initiates the AMPK/HIF-2α/VEGF/VEGFR2 axis, which orchestrates an expansion of the vasculature within obese adipose tissue. Consequently, this phenomenon leads to a significantly improved local microenvironment in obese adipose tissue, resulting in reduced inflammation and a notable improvement of obesity-associated metabolic complications. Scale bar=100 μm. **B** and **D**, One-way ANOVA and Tukey post hoc test; **E**, repeated ANOVA and Bonferroni post hoc test; **F** through **I**, nonparametric test.

recognized not only for enhancing insulin sensitivity but also for promoting vascularity in AT, facilitating communication among adipocytes, adipocyte progenitor cells, and endothelial cells to stimulate the recoupling of adipogenesis and angiogenesis, thereby remodeling obese AT. Consistently, our data demonstrate an elevated adipogenic potential, particularly in sWAT with GSK3β deletion. This suggests that GSK3β deficiency may enhance vasculature, creating more niches for adipocyte progenitors and promoting adipogenesis. This indicates a preference for hyperplasia over hypertrophy in the sWAT of obese GSK3β^{ADKO} mice, resulting in improved metabolic benefits. In the eWAT, while the adipogenic potential of progenitor cells is not significantly enhanced, the decrease in hypertrophic cell numbers and the slight increase in smaller cells may be due to reduced inflammatory cell death in the eWAT of obese GSK3^{ADKO} mice, at least partially, leading to enhanced AT function. These findings not only account for the observed increase in the sWAT to eWAT ratio but also indicate that AT remodeling shifts unhealthy adipocyte function toward a healthier state in GSK3β^{ADKO} mice. Consequently, these processes lead to a reduction in inflammation, hypoxia, and fibrosis in the AT microenvironment, potentially enhancing insulin sensitivity and improving systemic metabolic outcomes.

Induced AT vasculature by the VEGF/VEGFR signaling pathway was reported to counteract obesity-associated metabolic disorders.[16,20,23,24] However, contradictory findings have emerged about the effects of anti-angiogenic agents on metabolism and obesity prevention in mouse models.[17,67,68] These discrepancies may be attributed to the widespread impact of these systemic inhibitory approaches on metabolically significant non-ATs, affecting energy expenditure and food intake, thereby influencing the entire body's metabolism. The consequences of angiogenic modulation also vary depending on context. Stimulated vascularization during AT expansion, as in our model, benefits metabolism and offers potent protective effects. Conversely, anti-angiogenic activity in preexisting obesity improves metabolism by eliminating dysfunctional proinflammatory adipocytes.[20] In addition, it has been reported that the microenvironmental context, rather than the total dosage of total VEGF, is a key determinant of whether VEGF-induced angiogenesis is normal or abnormal.[69] This further emphasizes the importance of changes in VEGF levels within the AT microenvironment, such as those reported herein, which may have varying effects on systemic metabolism. Notably, in our analysis, VEGF levels were all endogenous and presumably only affected by the local AT depletion of GSK3β. All other feedback systems were intact.

AT undergoes hypoxia in response to obesity. This hypoxic environment, similar to what is observed during tumor growth, is thought to induce the expression and release of pro-angiogenic factors, including VEGF, mediated by HIF-1α. However, in obese AT, the response to hypoxia via HIF-1α may be inadequate to facilitate compensatory angiogenic expansion.[53] Overexpression of HIF-1α in AT does not lead to a pro-angiogenic response or increased VEGF expression levels,[70] indicating that adipocytes may rely on alternative HIF-1α-independent mechanisms to induce VEGF expression and angiogenesis. Emerging research suggests that HIF-1α and HIF-2α have distinct target genes and play unique roles in cellular processes.[71–73] They differ in their functions and effects on metabolic diseases and AT homeostasis.[74–77] In AT, HIF-1α contributes to fibrosis, inflammation, and systemic metabolic disorders,[70,74,78,79] whereas HIF-2α may reduce inflammation and improve insulin resistance.[70,74,75,79,80] It is reasonable to suspect that HIF-1α and HIF-2α play distinct roles in regulating AT vasculature, potentially by regulating VEGF or through other mechanisms. Our study revealed that GSK3β deficiency in adipocytes may promote VEGF expression by regulating the expression and nuclear accumulation of HIF-2α.

Furthermore, our investigation uncovered that the inhibition of AMPK activity hindered the nuclear translocation of HIF-2α, which is triggered by the adipocyte-specific deficiency of GSK3β. The nuclear translocation of HIF-2α is a crucial event in the transcriptional regulation of its target genes, such as VEGF, in adipocytes. Our findings showed that HIF-2α enhances VEGF/VEGFR2 signaling, mediating interactions between adipocytes and neighboring endothelial cells to promote vascularization within AT. Previous studies have emphasized the importance of phosphorylation in the activation and subsequent nuclear translocation of HIF-2α.[61,62] Our results indicate that GSK3 inhibition or ablation results in increased HIF-2α phosphorylation, which is subsequently reduced upon AMPK inhibition. Given the limited availability of site-specific HIF-2α phosphorylation antibodies, we assessed the total phosphorylation levels of tyrosine, serine, and threonine residues of HIF-2α. However, it remains unclear whether AMPK directly phosphorylates HIF-2α or if other downstream effectors of AMPK mediate its phosphorylation. Further analyses are necessary to identify the specific phosphorylation site(s) of HIF-2α and to elucidate the underlying mechanisms involved in the modulation of different sites phosphorylated by GSK3β and other kinases.

In conclusion, our findings shed light on the significance of the novel GSK3β/AMPK/HIF-2α/VEGF/VEGFR2 cascade axis in mediating the crosstalk between adipocytes and endothelial cells within AT during obesity. This axis plays a crucial role in regulating vascularization and modulating the deteriorated microenvironment of obese AT, thereby influencing inflammation and insulin sensitivity. Our study highlights the potential therapeutic implications of targeting this signaling axis to combat obesity-related metabolic complications.

ARTICLE INFORMATION

Received July 08, 2024; revision received November 18, 2024; accepted November 20, 2024.

Affiliations

Department of Biomedical Sciences, Faculty of Health Sciences (L.W., J.L., P.T., D.Z., L.T., Y.W., L.D.), The Ministry of Education Frontiers Science Center for Precision Oncology (L.W., L.D.), and Proteomics, Metabolomics and Drug development core facility, Faculty of Health Sciences (L.W.), University of Macau, China. Lunenfeld-Tanenbaum Research Institute, Sinai Health and Department of Medical Biophysics, University of Toronto, Ontario, Canada (T.M., J.R.W.).

Acknowledgments

The authors thank the support from Animal core facility, Proteomics, Metabolomics, and drug development core facility, Bioimage and Stem cell core facility of Faculty of Health Sciences of University of Macau.

Author Contributions

L. Wang and L. Di conceived the project and designed the study. L. Wang, J. Li, and P. Tang performed most of the experiments. D. Zhu and Y. Wang assisted in RNA sequencing data analysis. L. Tai assisted in the mouse experiments. T. Miyata and J.R. Woodgett provided mice and conceptual advice. L. Wang, L. Di, and J.R. Woodgett wrote the manuscript. All authors discussed the results and commented on the manuscript.

Sources of Funding

This study is supported by the Science and Technology Development Fund (FDCT) of Macao SAR to L. Di (FDCT/0014/2018/A1, FDCT/0117/2018/A3, FDCT/0048/2022/A1, 0054/2022/AMJ), the Multi-Year Research Grant from the University of Macau to L. Di (MYRG2022-00173-FHS), the National Natural Science Foundation of China (NSFC 81772980) to L. Di, and Canadian Institutes of Health Research Foundation Grant to J.R. Woodgett.

Disclosures

None.

Supplemental Material

Supplementary Materials and Methods
Figures S1–S11
Major Resources Table
Uncut Gel Blots
Statistics Analysis Table
References 81–83

REFERENCES

1. Rosen ED, MacDougald OA. Adipocyte differentiation from the inside out. *Nat Rev Mol Cell Biol*. 2006;7:885–896. doi: 10.1038/nrm2066
2. Cao Y. Angiogenesis modulates adipogenesis and obesity. *J Clin Invest*. 2007;117:2362–2368. doi: 10.1172/JCI32239
3. Christiaens V, Lijnen HR. Angiogenesis and development of adipose tissue. *Mol Cell Endocrinol*. 2010;318:2–9. doi: 10.1016/j.mce.2009.08.006
4. Lijnen HR. Angiogenesis and obesity. *Cardiovasc Res*. 2008;78:286–293. doi: 10.1093/cvr/cvm007
5. Herold J, Kalucka J. Angiogenesis in adipose tissue: the interplay between adipose and endothelial cells. *Front Physiol*. 2020;11:624903. doi: 10.3389/fphys.2020.624903
6. Houstis N, Rosen ED, Lander ES. Reactive oxygen species have a causal role in multiple forms of insulin resistance. *Nature*. 2006;440:944–948. doi: 10.1038/nature04634
7. Ozcan U, Cao Q, Yilmaz E, Lee AH, Iwakoshi NN, Ozdelen E, Tuncman G, Gorgun C, Glimcher LH, Hotamisligil GS. Endoplasmic reticulum stress links obesity, insulin action, and type 2 diabetes. *Science*. 2004;306:457–461. doi: 10.1126/science.1103160
8. Hosogai N, Fukuhara A, Oshima K, Miyata Y, Tanaka S, Segawa K, Furukawa S, Tochino Y, Komuro R, Matsuda M, et al. Adipose tissue hypoxia in obesity and its impact on adipocytokine dysregulation. *Diabetes*. 2007;56:901–911. doi: 10.2337/db06-0911
9. Trayhurn P, Wang B, Wood IS. Hypoxia in adipose tissue: a basis for the dysregulation of tissue function in obesity? *Br J Nutr*. 2008;100:227–235. doi: 10.1017/S0007114508971282
10. Trayhurn P. Hypoxia and adipose tissue function and dysfunction in obesity. *Physiol Rev*. 2013;93:1–21. doi: 10.1152/physrev.00017.2012
11. Yilmaz E. Endoplasmic reticulum stress and obesity. *Adv Exp Med Biol*. 2017;960:261–276. doi: 10.1007/978-3-319-48382-5_11
12. Sun K, Kusminski CM, Scherer PE. Adipose tissue remodeling and obesity. *J Clin Invest*. 2011;121:2094–2101. doi: 10.1172/JCI45887
13. Yilmaz M, Hotamisligil GS. Damned if you do, damned if you don't: the conundrum of adipose tissue vascularization. *Cell Metab*. 2013;17:7–9. doi: 10.1016/j.cmet.2012.12.014
14. Lumeng CN, Saltiel AR. Inflammatory links between obesity and metabolic disease. *J Clin Invest*. 2011;121:2111–2117. doi: 10.1172/JCI57132
15. Sung HK, Doh KO, Son JE, Park JG, Bae Y, Choi S, Nelson SM, Cowling R, Nagy K, Michael IP, et al. Adipose vascular endothelial growth factor regulates metabolic homeostasis through angiogenesis. *Cell Metab*. 2013;17:61–72. doi: 10.1016/j.cmet.2012.12.010
16. Robciuc MR, Kivela R, Williams IM, de Boer JF, van Dijk TH, Elamaa H, Tigistu-Sahle F, Molotkov D, Leppanen VM, Kakela R, et al. VEGFB/VEGFR1-induced expansion of adipose vasculature counteracts obesity and related metabolic complications. *Cell Metab*. 2016;23:712–724. doi: 10.1016/j.cmet.2016.03.004
17. Cao Y. Adipose tissue angiogenesis as a therapeutic target for obesity and metabolic diseases. *Nat Rev Drug Discov*. 2010;9:107–115. doi: 10.1038/nrd3055
18. Ioannidou A, Fisher RM, Hagberg CE. The multifaceted roles of the adipose tissue vasculature. *Obes Rev*. 2021;23:e13403. doi: 10.1111/obr.13403
19. Lijnen HR, Christiaens V, Scroyen I, Voros G, Tjwa M, Carmeliet P, Collen D. Impaired adipose tissue development in mice with inactivation of placental growth factor function. *Diabetes*. 2006;55:2698–2704. doi: 10.2337/db06-0526
20. Sun K, Wernstedt Asterholm I, Kusminski CM, Bueno AC, Wang ZV, Pollard JW, Brekken RA, Scherer PE. Dichotomous effects of VEGF-A on adipose tissue dysfunction. *Proc Natl Acad Sci USA*. 2012;109:5874–5879. doi: 10.1073/pnas.1200447109
21. Pasarica M, Sereda OR, Redman LM, Albarado DC, Hymel DT, Roan LE, Rood JC, Burk DH, Smith SR. Reduced adipose tissue oxygenation in human obesity: evidence for rarefaction, macrophage chemotaxis, and inflammation without an angiogenic response. *Diabetes*. 2009;58:718–725. doi: 10.2337/db08-1098
22. Fain JN, Madan AK, Hiler ML, Cheema P, Bahouth SW. Comparison of the release of adipokines by adipose tissue, adipose tissue matrix, and adipocytes from visceral and subcutaneous abdominal adipose tissues of obese humans. *Endocrinology*. 2004;145:2273–2282. doi: 10.1210/en.2003-1336
23. Park J, Kim M, Sun K, An YA, Gu X, Scherer PE. VEGF-A-expressing adipose tissue shows rapid beiging and enhanced survival after transplantation and confers IL-4-independent metabolic improvements. *Diabetes*. 2017;66:1479–1490. doi: 10.2337/db16-1081
24. Elias I, Franckhauser S, Ferre T, Vila L, Tafuro S, Munoz S, Roca C, Ramos D, Pujol A, Riu E, et al. Adipose tissue overexpression of vascular endothelial growth factor protects against diet-induced obesity and insulin resistance. *Diabetes*. 2012;61:1801–1813. doi: 10.2337/db11-0832
25. Cohen P, Frame S. The renaissance of GSK3. *Nat Rev Mol Cell Biol*. 2001;2:769–776. doi: 10.1038/35096075
26. Cormier KW, Woodgett JR. Recent advances in understanding the cellular roles of GSK-3. *F1000Res*. 2017;6:F1000 Faculty Rev–F1000 Faculty 167. doi: 10.12688/f1000research.10557.1
27. Frame S, Cohen P. GSK3 takes centre stage more than 20 years after its discovery. *Biochem J*. 2001;359:1–16. doi: 10.1042/0264-6021:3590001
28. Eldar-Finkelman H. Glycogen synthase kinase 3: an emerging therapeutic target. *Trends Mol Med*. 2002;8:126–132. doi: 10.1016/s1471-4914(01)02266-3
29. Wang L, Li J, Di LJ. Glycogen synthesis and beyond, a comprehensive review of GSK3 as a key regulator of metabolic pathways and a therapeutic target for treating metabolic diseases. *Med Res Rev*. 2022;42:946–982. doi: 10.1002/med.21867
30. Grimes CA, Jope RS. The multifaceted roles of glycogen synthase kinase 3beta in cellular signaling. *Prog Neurobiol*. 2001;65:391–426. doi: 10.1016/s0301-0082(01)00011-9
31. Doble BW, Woodgett JR. GSK-3: tricks of the trade for a multi-tasking kinase. *J Cell Sci*. 2003;116:1175–1186. doi: 10.1242/jcs.00384
32. MacAulay K, Doble BW, Patel S, Hansotia T, Sinclair EM, Drucker DJ, Nagy A, Woodgett JR. Glycogen synthase kinase 3alpha-specific regulation of murine hepatic glycogen metabolism. *Cell Metab*. 2007;6:329–337. doi: 10.1016/j.cmet.2007.08.013

33. Patel S, Macaulay K, Woodgett JR. Tissue-specific analysis of glycogen synthase kinase-3alpha (GSK-3alpha) in glucose metabolism: effect of strain variation. *PLoS One*. 2011;6:e15845. doi: 10.1371/journal.pone.0015845
34. Patel S, Doble BW, MacAulay K, Sinclair EM, Drucker DJ, Woodgett JR. Tissue-specific role of glycogen synthase kinase 3beta in glucose homeostasis and insulin action. *Mol Cell Biol*. 2008;28:6314–6328. doi: 10.1128/MCB.00763-08
35. Wang L, Wang Y, Zhang C, Li J, Meng Y, Dou M, Noguchi CT, Di L. Inhibiting glycogen synthase kinase 3 reverses obesity-induced white adipose tissue inflammation by regulating apoptosis inhibitor of macrophage/CD5L-mediated macrophage migration. *Arterioscler Thromb Vasc Biol*. 2018;38:2103–2116. doi: 10.1161/ATVBAHA.118.311363
36. Eldar-Finkelman H. Glycogen synthase kinase-3--a promising therapeutic target: Dr Hagit Eldar-Finkelman interviewed by Emma Quigley. *Expert Opin Ther Targets*. 2006;10:199–201. doi: 10.1517/14728222.10.2.199
37. Azoulay-Alfaguter I, Elya R, Avrahami L, Katz A, Eldar-Finkelman H. Combined regulation of mTORC1 and lysosomal acidification by GSK-3 suppresses autophagy and contributes to cancer cell growth. *Oncogene*. 2015;34:4613–4623. doi: 10.1038/onc.2014.390
38. McCamphill PK, Stoppel LJ, Senter RK, Lewis MC, Heynen AJ, Stoppel DC, Sridhar V, Collins KA, Shi X, Pan JQ, et al. Selective inhibition of glycogen synthase kinase 3alpha corrects pathophysiology in a mouse model of fragile X syndrome. *Sci Transl Med*. 2020;12:eaam8572. doi: 10.1126/scitranslmed.aam8572
39. Wagner FF, Benajiba L, Campbell AJ, Weiwer M, Sacher JR, Gale JP, Ross L, Puissant A, Alexe G, Conway A, et al. Exploiting an Asp-Glu "switch" in glycogen synthase kinase 3 to design paralog-selective inhibitors for use in acute myeloid leukemia. *Sci Transl Med*. 2018;10:eaam8460. doi: 10.1126/scitranslmed.aam8460
40. Coghlan MP, Culbert AA, Cross DA, Corcoran SL, Yates JW, Pearce NJ, Rausch OL, Murphy GJ, Carter PS, Roxbee Cox L, et al. Selective small molecule inhibitors of glycogen synthase kinase-3 modulate glycogen metabolism and gene transcription. *Chem Biol*. 2000;7:793–803. doi: 10.1016/s1074-5521(00)00025-9
41. Cross DA, Culbert AA, Chalmers KA, Facci L, Skaper SD, Reith AD. Selective small-molecule inhibitors of glycogen synthase kinase-3 activity protect primary neurones from death. *J Neurochem*. 2001;77:94–102. doi: 10.1046/j.1471-4159.2001.t01-1-00251.x
42. Stern JH, Rutkowski JM, Scherer PE. Adiponectin, leptin, and fatty acids in the maintenance of metabolic homeostasis through adipose tissue crosstalk. *Cell Metab*. 2016;23:770–784. doi: 10.1016/j.cmet.2016.04.011
43. Yamauchi T, Kamon J, Waki H, Terauchi Y, Kubota N, Hara K, Mori Y, Ide T, Murakami K, Tsuboyama-Kasaoka N, et al. The fat-derived hormone adiponectin reverses insulin resistance associated with both lipoatrophy and obesity. *Nat Med*. 2001;7:941–946. doi: 10.1038/90984
44. Kim JY, van de Wall E, Laplante M, Azzara A, Trujillo ME, Hofmann SM, Schraw T, Durand JL, Li H, Li G, et al. Obesity-associated improvements in metabolic profile through expansion of adipose tissue. *J Clin Invest*. 2007;117:2621–2637. doi: 10.1172/JCI31021
45. Aprahamian TR. Elevated adiponectin expression promotes adipose tissue vascularity under conditions of diet-induced obesity. *Metabolism*. 2013;62:1730–1738. doi: 10.1016/j.metabol.2013.07.010
46. Yamauchi T, Nio Y, Maki T, Kobayashi M, Takazawa T, Iwabu M, Okada-Iwabu M, Kawamoto S, Kubota N, Kubota T, et al. Targeted disruption of AdipoR1 and AdipoR2 causes abrogation of adiponectin binding and metabolic actions. *Nat Med*. 2007;13:332–339. doi: 10.1038/nm1557
47. Olefsky JM, Glass CK. Macrophages, inflammation, and insulin resistance. *Annu Rev Physiol*. 2010;72:219–246. doi: 10.1146/annurev-physiol-021909-135846
48. Tran TT, Yamamoto Y, Gesta S, Kahn CR. Beneficial effects of subcutaneous fat transplantation on metabolism. *Cell Metab*. 2008;7:410–420. doi: 10.1016/j.cmet.2008.04.004
49. Tanko LB, Bagger YZ, Alexandersen P, Larsen PJ, Christiansen C. Peripheral adiposity exhibits an independent dominant antiatherogenic effect in elderly women. *Circulation*. 2003;107:1626–1631. doi: 10.1161/01.CIR.0000057974.74060.68
50. McLaughlin T, Craig C, Liu LF, Perelman D, Allister C, Spielman D, Cushman SW. Adipose cell size and regional fat deposition as predictors of metabolic response to overfeeding in insulin-resistant and insulin-sensitive humans. *Diabetes*. 2016;65:1245–1254. doi: 10.2337/db15-1213
51. Ghaben AL, Scherer PE. Adipogenesis and metabolic health. *Nat Rev Mol Cell Biol*. 2019;20:242–258. doi: 10.1038/s41580-018-0093-z
52. Tang W, Zeve D, Suh JM, Bosnakovski D, Kyba M, Hammer RE, Tallquist MD, Graff JM. White fat progenitor cells reside in the adipose vasculature. *Science*. 2008;322:583–586. doi: 10.1126/science.1156232
53. Corvera S, Gealekman O. Adipose tissue angiogenesis: impact on obesity and type-2 diabetes. *Biochim Biophys Acta*. 2014;1842:463–472. doi: 10.1016/j.bbadis.2013.06.003
54. Strissel KJ, Stancheva Z, Miyoshi H, Perfield JW 2nd, DeFuria J, Jick Z, Greenberg AS, Obin MS. Adipocyte death, adipose tissue remodeling, and obesity complications. *Diabetes*. 2007;56:2910–2918. doi: 10.2337/db07-0767
55. Shibuya M. Vascular endothelial growth factor and its receptor system: physiological functions in angiogenesis and pathological roles in various diseases. *J Biochem*. 2013;153:13–19. doi: 10.1093/jb/mvs136
56. Bry M, Kivela R, Leppanen VM, Alitalo K. Vascular endothelial growth factor-B in physiology and disease. *Physiol Rev*. 2014;94:779–794. doi: 10.1152/physrev.00028.2013
57. Lal N, Puri K, Rodrigues B. Vascular endothelial growth factor B and its signaling. *Front Cardiovasc Med*. 2018;5:39. doi: 10.3389/fcvm.2018.00039
58. Abel ED, Peroni O, Kim JK, Kim YB, Boss O, Hadro E, Minnemann T, Shulman GI, Kahn BB. Adipose-selective targeting of the GLUT4 gene impairs insulin action in muscle and liver. *Nature*. 2001;409:729–733. doi: 10.1038/35055575
59. Wang GL, Jiang BH, Rue EA, Semenza GL. Hypoxia-inducible factor 1 is a basic-helix-loop-helix-PAS heterodimer regulated by cellular O2 tension. *Proc Natl Acad Sci U S A*. 1995;92:5510–5514. doi: 10.1073/pnas.92.12.5510
60. Wallace EM, Rizzi JP, Han G, Wehn PM, Cao Z, Du X, Cheng T, Czerwinski RM, Dixon DD, Goggin BS, et al. A small-molecule antagonist of HIF2alpha is efficacious in preclinical models of renal cell carcinoma. *Cancer Res*. 2016;76:5491–5500. doi: 10.1158/0008-5472.CAN-16-0473
61. Conrad PW, Freeman TL, Beitner-Johnson D, Millhorn DE. EPAS1 trans-activation during hypoxia requires p42/p44 MAPK. *J Biol Chem*. 1999;274:33709–33713. doi: 10.1074/jbc.274.47.33709
62. Gkotinakou IM, Befani C, Simos G, Liakos P. ERK1/2 phosphorylates HIF-2alpha and regulates its activity by controlling its CRM1-dependent nuclear shuttling. *J Cell Sci*. 2019;132:jcs225698. doi: 10.1242/jcs.225698
63. Gustafson B, Gogg S, Hedjazifar S, Jenndahl L, Hammarstedt A, Smith U. Inflammation and impaired adipogenesis in hypertrophic obesity in man. *Am J Physiol Endocrinol Metab*. 2009;297:E999–E1003. doi: 10.1152/ajpendo.00377.2009
64. Kim SM, Lun M, Wang M, Senyo SE, Guillermier C, Patwari P, Steinhauser ML. Loss of white adipose hyperplastic potential is associated with enhanced susceptibility to insulin resistance. *Cell Metab*. 2014;20:1049–1058. doi: 10.1016/j.cmet.2014.10.010
65. Vishvanath L, Gupta RK. Contribution of adipogenesis to healthy adipose tissue expansion in obesity. *J Clin Invest*. 2019;129:4022–4031. doi: 10.1172/JCI129191
66. Sakers A, De Siqueira MK, Seale P, Villanueva CJ. Adipose-tissue plasticity in health and disease. *Cell*. 2022;185:419–446. doi: 10.1016/j.cell.2021.12.016
67. Brakenhielm E, Cao R, Gao B, Angelin B, Cannon B, Parini P, Cao Y. Angiogenesis inhibitor, TNP-470, prevents diet-induced and genetic obesity in mice. *Circ Res*. 2004;94:1579–1588. doi: 10.1161/01.RES.0000132745.76882.70
68. Rupnick MA, Panigrahy D, Zhang CY, Dallabrida SM, Lowell BB, Langer R, Folkman MJ. Adipose tissue mass can be regulated through the vasculature. *Proc Natl Acad Sci USA*. 2002;99:10730–10735. doi: 10.1073/pnas.162349799
69. Ozawa CR, Banfi A, Glazer NL, Thurston G, Springer ML, Kraft PE, McDonald DM, Blau HM. Microenvironmental VEGF concentration, not total dose, determines a threshold between normal and aberrant angiogenesis. *J Clin Invest*. 2004;113:516–527. doi: 10.1172/JCI18420
70. Halberg N, Khan T, Trujillo ME, Wernstedt-Asterholm I, Attie AD, Sherwani S, Wang ZV, Landskroner-Eiger S, Dineen S, Magalang UJ, et al. Hypoxia-inducible factor 1alpha induces fibrosis and insulin resistance in white adipose tissue. *Mol Cell Biol*. 2009;29:4467–4483. doi: 10.1128/MCB.00192-09
71. Hu CJ, Iyer S, Sataur A, Covello KL, Chodosh LA, Simon MC. Differential regulation of the transcriptional activities of hypoxia-inducible factor 1 alpha (HIF-1alpha) and HIF-2alpha in stem cells. *Mol Cell Biol*. 2006;26:3514–3526. doi: 10.1128/MCB.26.9.3514-3526.2006
72. Hu CJ, Wang LY, Chodosh LA, Keith B, Simon MC. Differential roles of hypoxia-inducible factor 1alpha (HIF-1alpha) and HIF-2alpha in hypoxic gene regulation. *Mol Cell Biol*. 2003;23:9361–9374. doi: 10.1128/MCB.23.24.9361-9374.2003
73. Dengler VL, Galbraith M, Espinosa JM. Transcriptional regulation by hypoxia inducible factors. *Crit Rev Biochem Mol Biol*. 2014;49:1–15. doi: 10.3109/10409238.2013.838205
74. Jiang C, Qu A, Matsubara T, Chanturiya T, Jou W, Gavrilova O, Shah YM, Gonzalez FJ. Disruption of hypoxia-inducible factor 1 in adipocytes improves

insulin sensitivity and decreases adiposity in high-fat diet-fed mice. *Diabetes*. 2011;60:2484–2495. doi: 10.2337/db11-0174
75. Lee YS, Kim JW, Osborne O, Oh DY, Sasik R, Schenk S, Chen A, Chung H, Murphy A, Watkins SM, et al. Increased adipocyte O2 consumption triggers HIF-1alpha, causing inflammation and insulin resistance in obesity. *Cell*. 2014;157:1339–1352. doi: 10.1016/j.cell.2014.05.012
76. Garcia-Martin R, Alexaki VI, Qin N, Rubin de Celis MF, Economopoulou M, Ziogas A, Gercken B, Kotlabova K, Phieler J, Ehrhart-Bornstein M, et al. Adipocyte-specific hypoxia-inducible factor 2alpha deficiency exacerbates obesity-induced brown adipose tissue dysfunction and metabolic dysregulation. *Mol Cell Biol*. 2016;36:376–393. doi: 10.1128/MCB.00430-15
77. Takikawa A, Mahmood A, Nawaz A, Kado T, Okabe K, Yamamoto S, Aminuddin A, Senda S, Tsuneyama K, Ikutani M, et al. HIF-1alpha in myeloid cells promotes adipose tissue remodeling toward insulin resistance. *Diabetes*. 2016;65:3649–3659. doi: 10.2337/db16-0012
78. Shin MK, Drager LF, Yao Q, Bevans-Fonti S, Yoo DY, Jun JC, Aja S, Bhanot S, Polotsky VY. Metabolic consequences of high-fat diet are attenuated by suppression of HIF-1alpha. *PLoS One*. 2012;7:e46562. doi: 10.1371/journal.pone.0046562
79. Sun K, Halberg N, Khan M, Magalang UJ, Scherer PE. Selective inhibition of hypoxia-inducible factor 1alpha ameliorates adipose tissue dysfunction. *Mol Cell Biol*. 2013;33:904–917. doi: 10.1128/MCB.00951-12
80. Zhang X, Zhang Y, Wang P, Zhang SY, Dong Y, Zeng G, Yan Y, Sun L, Wu Q, Liu H, et al. Adipocyte hypoxia-inducible factor 2alpha suppresses atherosclerosis by promoting adipose ceramide catabolism. *Cell Metab*. 2019;30:937–951.e5. doi: 10.1016/j.cmet.2019.09.016
81. Wang L, Wang Y, Meng Y, Zhang C, Di L. GSK3-activated STAT5 regulates expression of SFRPs to modulate adipogenesis. *FASEB J*. 2018;32:4714–4726. doi: 10.1096/fj.201701314r
82. DeCicco-Skinner KL, Henry GH, Cataisson C, Tabib T, Gwilliam JC, Watson NJ, Bullwinkle EM, Falkenburg L, O'Neill RC, Morin A, et al. Endothelial cell tube formation assay for the in vitro study of angiogenesis. *J Vis Exp*. 2014;91:e51312. doi: 10.3791/51312
83. Jiang Y, Lan-Hing Yeung J, Lee JH, An J, Steadman PE, Kim JR, Sung HK. Visualization of 3D white adipose tissue structure using whole-mount staining. *J Vis Exp*. 2018;141:e58683. doi: 10.3791/58683